https://doi.org/10.1093/plcell/koad170 THE PLANT CELL 2023: 1–19

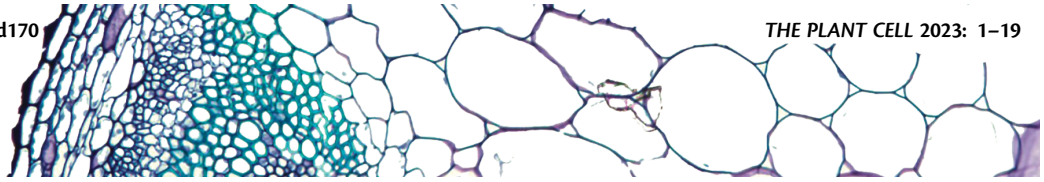

Research Article

MYB112 connects light and circadian clock signals to promote hypocotyl elongation in Arabidopsis

Yupeng Cai [1,2,†] Yongting Liu [1,†] Yangyang Fan [3] Xitao Li [1,4] Maosheng Yang [1] Dongqing Xu [5] Haiyang Wang [6] Xing Wang Deng [1,7,*] and Jian Li [1,*]

1 Key Laboratory of Molecular Design for Plant Cell Factory of Guangdong Higher Education Institutes, Institute of Plant and Food Science, Department of Biology, School of Life Sciences, Southern University of Science and Technology, Shenzhen 518055, China
2 National Center for Transgenic Research in Plants, Institute of Crop Sciences, Chinese Academy of Agricultural Sciences, Beijing 100081, China
3 Institute of Plant Protection, Beijing Academy of Agriculture and Forestry Sciences, Beijing Engineering Research Center for Edible Mushroom, Beijing 100097, China
4 School of Life Science, Huizhou University, Huizhou 516007, China
5 State Key Laboratory of Crop Genetics and Germplasm Enhancement, National Center for Soybean Improvement, College of Agriculture, Nanjing Agricultural University, Nanjing 210095, China
6 State Key Laboratory for Conservation and Utilization of Subtropical Agro-Bioresources, South China Agricultural University, Guangzhou 510642, China
7 State Key Laboratory of Protein and Plant Gene Research, Peking–Tsinghua Center for Life Sciences, School of Advanced Agriculture Sciences and School of Life Sciences, Peking University, Beijing 100871, China

*Author for correspondence: deng@pku.edu.cn (X.W.D.), lixiujian@yeah.net (J.L.)
†These authors contributed equally to this work.
The author(s) responsible for distribution of materials integral to the findings presented in this article in accordance with the policy described in the Instructions for Authors (https://academic.oup.com/plcell/pages/General-Instructions) is (are): Jian Li (lixiujian@yeah.net).

Abstract

Ambient light and the endogenous circadian clock play key roles in regulating Arabidopsis (*Arabidopsis thaliana*) seedling photomorphogenesis. *PHYTOCHROME-INTERACTING FACTOR 4* (*PIF4*) acts downstream of both light and the circadian clock to promote hypocotyl elongation. Several members of the R2R3-MYB transcription factor (TF) family, the most common type of MYB TF family in Arabidopsis, have been shown to be involved in regulating photomorphogenesis. Nonetheless, whether R2R3-MYB TFs are involved in connecting the light and clock signaling pathways during seedling photomorphogenesis remains unknown. Here, we report that MYB112, a member of the R2R3-MYB family, acts as a negative regulator of seedling photomorphogenesis in Arabidopsis. The light signal promotes the transcription and protein accumulation of MYB112. *myb112* mutants exhibit short hypocotyls in both constant light and diurnal cycles. MYB112 physically interacts with PIF4 to enhance the transcription of PIF4 target genes involved in the auxin pathway, including *YUCCA8* (*YUC8*), *INDOLE-3-ACETIC ACID INDUCIBLE 19* (*IAA19*), and *IAA29*. Furthermore, MYB112 directly binds to the promoter of *LUX ARRHYTHMO* (*LUX*), the central component of clock oscillators, to repress its expression mainly in the afternoon and relieve LUX-inhibited expression of *PIF4*. Genetic evidence confirms that *LUX* acts downstream of *MYB112* in regulating hypocotyl elongation. Thus, the enhanced transcript accumulation and transcriptional activation activity of PIF4 by MYB112 additively promotes the expression of auxin-related genes, thereby increasing auxin synthesis and signaling and fine-tuning hypocotyl growth under diurnal cycles.

Introduction

As one of the most important environmental signals for plants, light plays a key role in seedling morphogenesis. While germinating under soil without light, Arabidopsis (*Arabidopsis thaliana*) seedlings undergo skotomorphogenesis, characterized by rapid elongation of the hypocotyl,

Received January 20, 2023. Accepted June 13, 2023. Advance access publication June 19, 2023

closed cotyledons, and an apical hook. Upon reaching the light, the seedlings undergo photomorphogenesis, characterized by inhibited elongation of the hypocotyl, opened cotyledons, and the disappearance of the apical hook (Chory et al. 1989; Deng et al. 1991; Martinez-Garcia et al. 2000; Jiao et al. 2007). One of the most remarkable events of light-controlled morphogenesis is hypocotyl elongation (McNellis and Deng 1995). Accelerated hypocotyl elongation in the dark helps seedlings reach sunlight, while the inhibition of hypocotyl elongation by light signals prevents them from lodging (Shi et al. 2018).

In Arabidopsis, different receptors have evolved that perceive different wavelengths of sunlight (Vierstra and Quail 1983; Sharrock and Quail 1989; Lin et al. 1995; Rizzini et al. 2011; Christie et al. 2012). Photoreceptors activated by light repress the functions of central negative regulators to release the functions of light-responsive transcription factors (TFs) and thereby promote photomorphogenesis (Jiao et al. 2007). PHYTOCHROME-INTERACTING FACTORS (PIFs), a small subset of the basic helix-loop-helix (bHLH) TF family, are major repressors of photomorphogenesis (Martinez-Garcia et al. 2000; Huq and Quail 2002; Leivar et al. 2008b; Shin et al. 2009). Arabidopsis possesses 8 PIFs (PIF1–PIF8) (Leivar and Quail 2011; Pham et al. 2018a). Genetic analysis shows that the quadruple mutant *pifq*, which lacks *PIF1*, *PIF3*, *PIF4*, and *PIF5* in Arabidopsis, exhibits constitutive photomorphogenesis in the dark (Leivar et al. 2008b; Shin et al. 2009). PIF proteins accumulate in large amounts in dark-grown seedlings (Bauer et al. 2004; Shen et al. 2007; Pham et al. 2018b). These proteins can bind to the G-box and E-box *cis*-elements to regulate the expression of numerous target genes (Martinez-Garcia et al. 2000; Shin et al. 2007; Franklin et al. 2011), thereby inhibiting photomorphogenesis in the dark. When seedlings are switched from dark to light, photoactivated phytochrome B rapidly induces phosphorylation of PIFs in a PHOTOREGULATORY PROTEIN KINASE (PPK)-dependent manner (Al-Sady et al. 2006; Ni et al. 2017). PIFs are subsequently polyubiquitinated and degraded via the 26S proteasome pathway. Two types of E3 ubiquitin ligases, LIGHT-RESPONSE BRIC-A-BRACK/TRAMTRACK/BROAD ligases (LRBs) and EIN3-BINDING F-BOX PROTEINS (EBFs), are involved in light-induced ubiquitination and degradation of PIF3 (Christians et al. 2012; Ni et al. 2014; Dong et al. 2017). Interestingly, the protein levels of several PIFs, such as PIF4, can also reaccumulate in prolonged red light, thereby moderately inhibiting photomorphogenesis by modulating phyB protein levels (Leivar et al. 2008a; Yan et al. 2020). Notable target genes of PIF4 function in promoting hypocotyl elongation are mainly involved in auxin biosynthesis and signal transduction (Franklin et al. 2011; Hornitschek et al. 2012; Sun et al. 2012). PIF4 can directly bind to the G-box *cis*-element of *YUCCA8*, a gene for auxin biosynthesis, to transactivate its expression, thereby increasing the level of endogenous auxin and accelerating hypocotyl elongation (Hornitschek et al. 2012; Sun et al. 2012; Huai et al. 2018; Han et al. 2019; Zhou et al. 2019; Gao et al. 2022). PIF4 also enables CYCLING DOF FACTOR 2 (CDF2) to activate *YUCCA8* expression by enhancing DNA binding of CDF2 (Gao et al. 2022). PIF4 also directly activates the expression of *IAA19* and *IAA29* to sustain hypocotyl elongation in the presence of persistent shade (Sun et al. 2013; Pucciariello et al. 2018).

In addition to the auxin signaling mentioned above, the intrinsic circadian clock *in planta* also functions as one of the major endogenous signals involved in the regulation of photomorphogenesis. It can adjust the growth of Arabidopsis to the day–night cycle, thus optimizing the environmental adaptation of Arabidopsis (Nozue et al. 2007; Nusinow et al. 2011; Su et al. 2021; Xu et al. 2022). The circadian clock mainly consists of the input pathways, the central oscillator, and the output pathways. The central oscillator is used to receive input signals and generate rhythmic output signals (Xu et al. 2022). The oscillator consists of a set of transcriptionals–translational feedback loops (TTFLs) that include morning-phased and evening-phased genes. Central oscillator genes are expressed at different times of a day and can affect the expression and/or activities of each other as well as of genes acting in output pathways (Schaffer et al. 1998; Wang and Tobin 1998; Makino et al. 2001; Mizuno and Nakamichi 2005; Nusinow et al. 2011; Herrero et al. 2012; Huang et al. 2012; Kamioka et al. 2016). Morning-phased genes mainly include two homologous MYB TFs: *CIRCADIAN CLOCK ASSOCIATED1* (*CCA1*) and *LATE ELONGATED HYPOCOTYL* (*LHY*) (Schaffer et al. 1998; Wang and Tobin 1998), whereas evening-phased genes mainly include *EARLY FLOWERING3* (ELF3), *EARLY FLOWERING4* (*ELF4*), and *LUX ARRHYTHMO* (*LUX*) (Nusinow et al. 2011). The transcriptional regulatory complex formed by ELF3-ELF4-LUX is also known as the evening complex (EC) (Nusinow et al. 2011). LUX is a single-MYB-domain-containing TF in EC (Hazen et al. 2005; Nusinow et al. 2011). The morning complex CCA1/LHY can directly bind to the evening element in the *LUX* promoter to repress its expression (Hazen et al. 2005). CCA1/LHY can promote the expression of *PIF4* under diurnal cycles (Nozue et al. 2007; Sun et al. 2019). In contrast, LUX targets EC to the promoter of *PIF4* to repress *PIF4* expression in the early evening (Nusinow et al. 2011). Thus, simultaneous elevation of PIF4 mRNA and protein levels at dawn allows maximal prolongation of the hypocotyl under short-day conditions (Nusinow et al. 2011).

MYB TFs comprise one of the largest families of transcriptional regulators in plants (Ma and Constabel 2019). Among them, the R2R3-MYB TFs, which have 2 MYB repeats in their DNA-binding domain (BD), are widely involved in regulating plant-specific processes, including secondary metabolisms, response to biotic and abiotic stresses, etc. (Mengiste et al. 2003; Stracke et al. 2007; Dubos et al. 2010). The R2R3-MYB family in Arabidopsis includes 126 members (Millard et al. 2019). However, whether these genes are involved in the connection of light and clock signals during seedling photomorphogenesis is still completely unknown. The MYB112 is a member of the R2R3-MYB family (Lotkowska et al. 2015). Previous study has shown that high light stress induces transcription of *MYB112*. MYB112 regulates gene expression to promote

anthocyanin biosynthesis (Lotkowska et al. 2015). Here, we report that MYB112 promotes hypocotyl elongation in both constant light and diurnal cycles. The light signal promotes transcription and protein accumulation of MYB112. On the one hand, MYB112 binds to the promoter of *LUX* to repress its expression in the afternoon, which relieves LUX-inhibited expression of *PIF4*. On the other hand, MYB112 physically interacts with PIF4 to enhance transcription of PIF4's target genes. Thus, MYB112 connects light and clock signals to promote PIF4-induced transcription of auxin-related genes and fine-tuning hypocotyl growth under diurnal cycles.

Results

MYB112 negatively regulates photomorphogenesis in the light

A previous study has shown that MYB112 is involved in anthocyanin biosynthesis under high light stress (Lotkowska et al. 2015). To investigate the role of MYB112 in regulating seedling photomorphogenesis, we used the CLUSTERED REGULARLY INTERSPACED SHORT PALINDROMIC REPEAT/CRISPR-ASSOCIATED 9 (CRISPR/Cas9) system (Wang et al. 2015) to generate *myb112* mutants. We obtained 2 independent homozygous *myb112* mutants (Supplemental Fig. S1), which we designated *myb112-3* and *myb112-4* to distinguish them from the preexisting T-DNA mutants *myb112-1* and *myb112-2* (Lotkowska et al. 2015). We found that the hypocotyls of the *myb112* mutants were the same length as those of the wild type (Columbia-0 [Col-0]) in the dark (Supplemental Fig. S2), suggesting MYB112 has no effect on hypocotyl elongation in the dark. However, the hypocotyls of both *myb112* mutants were significantly shorter than those of Col-0 when grown under continuous white, red, far-red, and blue light (Fig. 1).

Next, we generated transgenic plants overexpressing *YFP-MYB112* driven by the cauliflower mosaic virus *35S* promoter. MYB112 mRNA and proteins in the *YFP-MYB112 #2* and *YFP-MYB112 #3* lines are detectable by reverse transcription quantitative PCR (RT-qPCR) and immunoblot analysis (Supplemental Fig. S3). These two transgenic lines overexpressing *YFP-MYB112* had the same hypocotyl length as Col-0 in the dark (Supplemental Fig. S2), whereas they had longer hypocotyls than Col-0 under different light conditions as indicated (Fig. 1). These genetic and phenotypic results confirm that MYB112 promotes hypocotyl elongation in the light and acts as a negative regulator of photomorphogenesis in Arabidopsis.

Transcriptome analysis of MYB112-regulated genes

To illustrate the molecular role of MYB112 in regulating photomorphogenesis in Arabidopsis, the global transcriptome differences between Col-0 and the *myb112-4* mutant were analyzed by RNA sequencing (RNA-seq). Col-0 and *myb112-4* seedlings grown for 4 d under continuous white light (23.61 μmol m^{-2} s^{-1}) were sampled for RNA-seq. We found that 788 genes were upregulated and 1,277 genes were downregulated in *myb112-4* versus Col-0 (Fig. 2A and Supplemental Data Set 1). Gene ontology (GO) analysis revealed that the downregulated genes in the *myb112-4* mutant were mainly involved in some biological processes, including red or far-red light signaling pathway, circadian rhythm, response to auxin, response to low light intensity stimulus, photosynthesis, light harvesting in photosystem I, and carboxylic acid catabolic process (Fig. 2B). Among these, we focused on three processes, red or far-red light signaling pathway, circadian rhythm, and response to auxin, which are closely related to photomorphogenesis. Intriguingly, we noticed that several *PIF* family genes, including *PIF3* and *PIF4*, and several genes involved in the auxin biosynthetic or signaling pathway, including *IAA19*, *IAA29*, *YUCCA7*, and *YUCCA8*, were downregulated in the *myb112-4* mutant versus Col-0 (Fig. 2, C and D, Supplemental Fig. S4). Therefore, we next examined the response of *myb112* mutants to exogenous auxin. Treatment with 0.1 μM 2,4-D led to a significant increase in hypocotyl elongation in *myb112* mutants and completely rescued the hypocotyl elongation defect of *myb112* mutants (Fig. 2E). These data provide further evidence that the short hypocotyl phenotype of *myb112* mutants is due to auxin deficiency.

MYB112 physically interacts with PIF4 to promote its transcriptional activation activity

Previous studies have shown that PIF4 promotes hypocotyl elongation in an auxin-dependent manner (Franklin et al. 2011; Sun et al. 2012; Huai et al. 2018). PIF4 can bind to the promoters of auxin pathway genes, such as the auxin biosynthesis gene *YUCCA8* and the auxin response genes *IAA19* and *IAA29*, and activate the expression of these genes (Hornitschek et al. 2012; Sun et al. 2012; Sun et al. 2013; Huai et al. 2018; Pucciariello et al. 2018; Han et al. 2019; Zhou et al. 2019; Gao et al. 2022). Transcriptome analysis showed that the expression of *PIF4* and its target genes, including *YUCCA8*, *IAA19*, and *IAA29*, decreased significantly in *myb112-4* (Fig. 2, C and D). We also used RT-qPCR to confirm the expression of these genes in *myb112* mutants and *YFP-MYB112* lines grown for 4 d under continuous white light conditions. As shown in Fig. 3A, the transcript level of *PIF4* was significantly lower in *myb112* mutants than in Col-0, whereas it was significantly higher in *YFP-MYB112* lines. Accordingly, the expression of *YUCCA8*, *IAA19*, and *IAA29* was lower in *myb112* mutants than in Col-0, whereas it was higher in *YFP-MYB112* lines (Fig. 3B, Supplemental Fig. S5, A and B). Because MYB112 has been previously described as a TF, these results suggest that MYB112 may promote the expression of *PIF4*, thereby enhancing the expression of these target genes of PIF4 in the light. However, the results of the yeast 1-hybrid (Y1H) assay showed that MYB112 was unable to directly bind to the promoter of *PIF4* in yeast cells (Supplemental Fig. S6A). In addition, while binding of PIF4 to the *YUCCA8* promoter was used as a positive control, MYB112 failed to bind directly to the *YUCCA8* promoter in

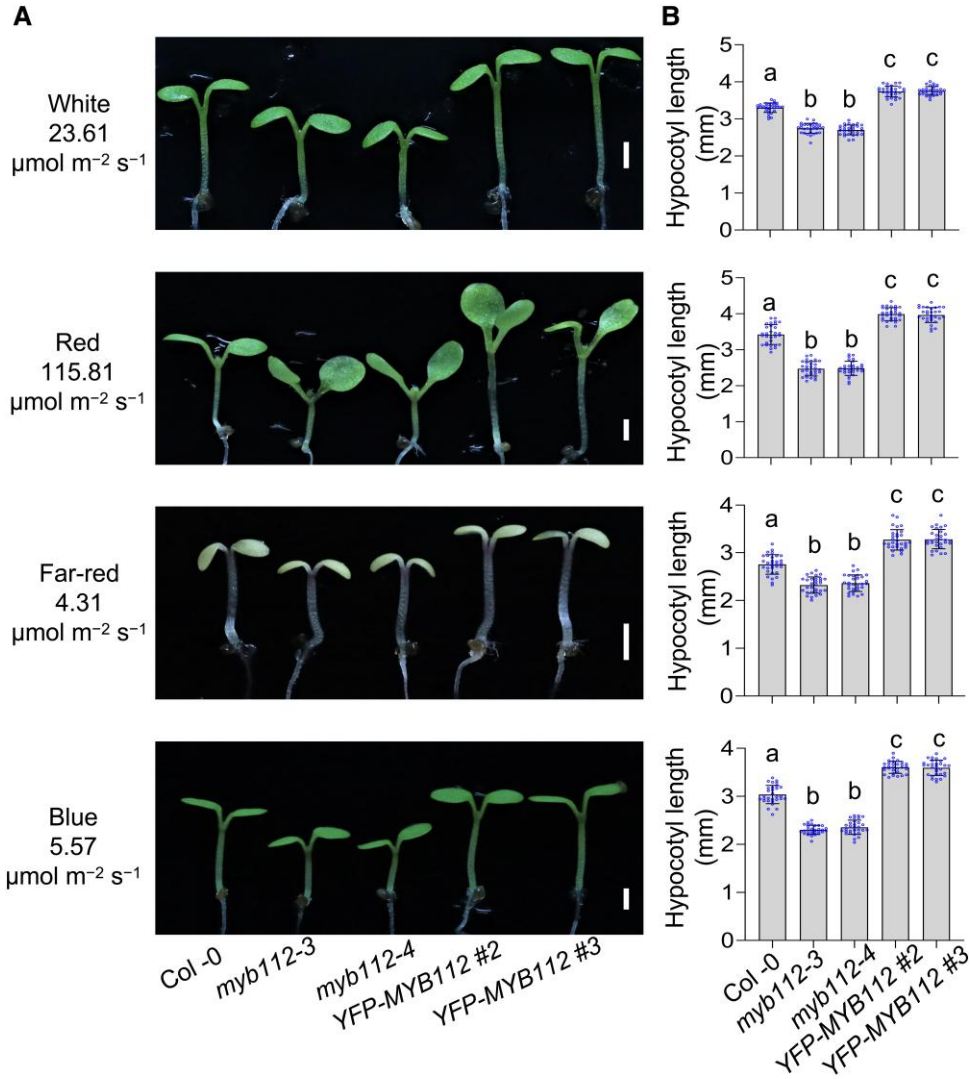

Figure 1. MYB112 suppress photomorphogenesis in the light. **A)** Hypocotyl phenotypes of Col-0, two *myb112* mutants, and two independent *MYB112* overexpression lines grown for 4 d under continuous light conditions. *YFP-MYB112*, transgenic plants overexpressing YFP-tagged MYB112. Scale bars, 1 mm. **B)** Hypocotyl lengths of Col-0, two *myb112* mutants, and two independent *MYB112* overexpression lines grown for 4 d under various light conditions. Data are presented as means ± SD, $n = 30$. Lowercase letters above the histogram represent statistically significant differences ($P < 0.05$) determined by one-way ANOVA with Tukey's post hoc analysis.

Y1H (Supplemental Fig. S6B). These results indicate that MYB112 is unable to bind directly to the promoters of *PIF4* or *YUCCA8*.

We next performed a yeast 2-hybrid (Y2H) assay to test whether MYB112 can directly interact with PIF4 protein. Full-length and truncated fragments of MYB112 were fused with the BD, and full-length PIF4 was fused with the activation domain (AD). Although full-length MYB112 exhibited self-activation in yeast cells, subsequent analysis of β-galactosidase activity revealed that full-length and N-terminal MYB112 could interact with PIF4 (Fig. 3C). To further verify the physical interaction between MYB112 and PIF4, we performed an in vitro pull-down assay. The result shows that MYB112 physically interacts with PIF4 in vitro (Fig. 3D). Subsequently, the in vivo interaction between MYB112 and PIF4 was confirmed using firefly luciferase complementation imaging (LCI) and coimmunoprecipitation (Co-IP) (Fig. 3, E and F). Taken together, these results demonstrate that MYB112 physically interacts with PIF4 in Arabidopsis.

Indeed, there are several lines of evidence that heterodimer combinations can enhance the transcriptional activity of TFs toward target genes. For example, the interaction of PIF4 and BRASSINAZOLE-RESISTANT 1 (BZR1) enhances its transcriptional activation activity toward the target gene *PACLOBUTRAZOL RESISTANCE 5* (*PRE5*) (Oh et al. 2012). We investigated the role of the interaction between MYB112 and PIF4 in regulating PIF4 activity using a transient expression assay in leaves of *Nicotiana benthamiana*. MYB112 alone failed to induce the expression of *YUCCA8*$_{pro}$*:LUC*,

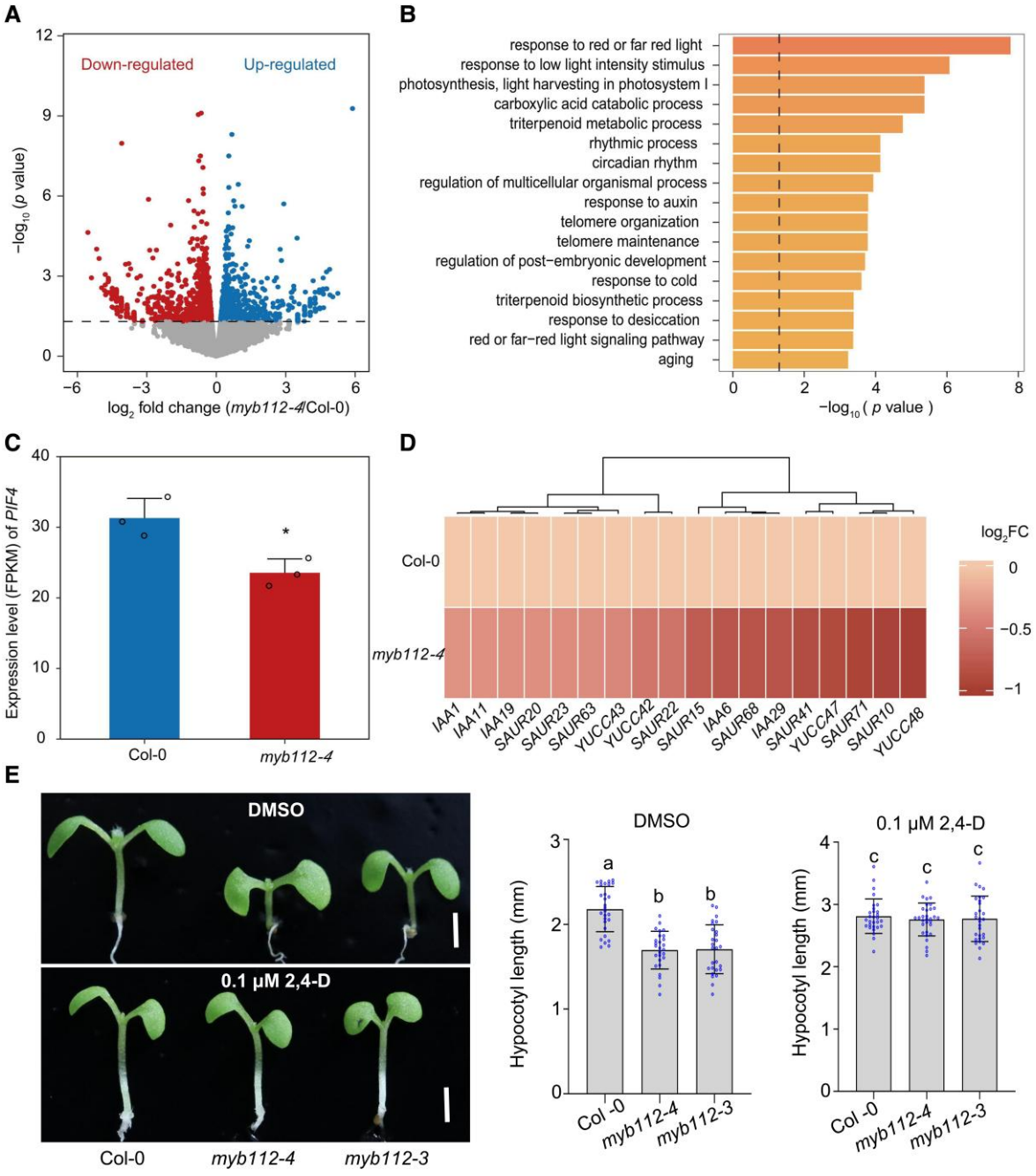

Figure 2. Transcriptome analysis of MYB112-regulated genes. **A)** Upregulated genes and downregulated genes in *myb112-4* mutant versus Col-0. Col-0 and *myb112-4* seedlings were grown under continuous white light (23.61 μmol m^{-2} s^{-1}) for 4 d before sampling. **B)** Top 17 GO term enrichments (biological process) for downregulated genes in *myb112-4*. The dashed line corresponds to the Benjamini–Hochberg adjusted *P* value = 0.05. **C)** Gene expression analysis of *PIF4* in *myb112-4* and Col-0. Asterisks represent statistically significant differences as determined by Student's *t*-test (**$P < 0.01$). **D)** Hierarchical clustering of various genes related to the auxin biosynthetic or signaling pathway in *myb112-4* mutant and Col-0. **E)** Hypocotyl phenotypes and lengths of Col-0 and *myb112* mutants treated with 0.1 μM 2,4-D. Scale bars, 1 mm. Data are presented as means ± SD, $n > 27$. Lowercase letters above the histogram represent statistically significant differences ($P < 0.05$) determined by one-way ANOVA with Tukey's post hoc analysis.

consistent with the previous finding that MYB112 did not bind to the *YUCCA8* promoter in yeast (Fig. 3G, Supplemental Fig. S6B). However, MYB112 was able to significantly enhance the transcriptional activation activity of PIF4 toward $YUCCA8_{pro}$:*LUC* when MYB112 and PIF4 were coexpressed in *N. benthamiana* leaves (Fig. 3G). Similarly, we found that MYB112 alone failed to induce the expression of $IAA19_{pro}$:*LUC* or $IAA29_{pro}$:*LUC* but was able to significantly

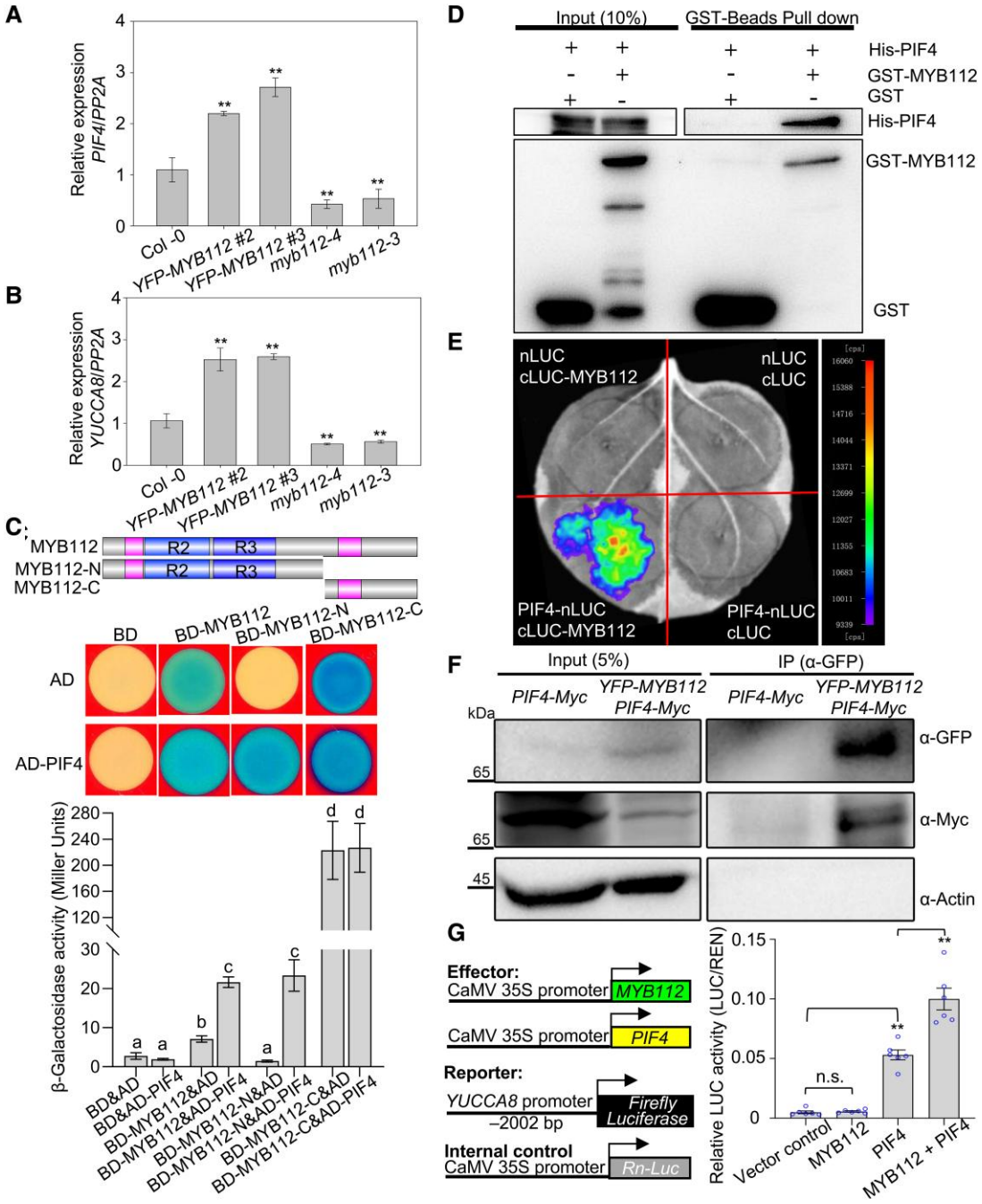

Figure 3. MYB112 physically interacts with PIF4 to promote *YUCCA8* expression. The relative expression of *PIF4* **A)** and *YUCCA8* **B)** in Col-0, *myb112* mutants, and *YFP-MYB112* lines was determined by RT-qPCR. Relative transcript levels were normalized to *PP2A*. Error bars represent SD of 3 technical replicates. Asterisks represent statistically significant differences in gene expression between *MYB112* materials and Col-0 (**$P < 0.01$), as determined by one-way ANOVA with Tukey's post hoc analysis. **C)** Interaction of MYB112 and PIF4 in the LexA-based yeast 2-hybrid system. BD, DNA-binding domain; AD, activation domain; MYB112-N, 1 to 170 aa; MYB112-C, 171 to 243 aa. The β-galactosidase activities of yeast cells were quantified by liquid culture assays using ONPG as the substrate. Results were presented as means ± SD, $n = 3$. Lowercase letters above the histogram represent statistically significant differences ($P < 0.01$) determined by one-way ANOVA with Tukey's post hoc analysis. **D)** In vitro pull-down assay showing the interaction between MYB112 and PIF4. MYB112 was fused with the GST-tag; PIF4 was fused with the His-tag. **E)** LCI assay showing the interaction between MYB112 and PIF4 in *N. benthamiana* leaves. nLUC, the vector containing the N-terminal fragment of firefly luciferase; cLUC, the vector containing the C-terminal fragment of firefly luciferase; cps, counts per second. **F)** Co-IP assay showing the association of MYB112 and PIF4 in vivo. YFP-MYB112 was immunoprecipitated with GFP-trap beads, and then, the pellet proteins were separated by SDS-PAGE and detected by immunoblot analysis with anti-GFP and anti-Myc antibodies. Actin was used as a loading control. **G)** Transient expression assay in *N. benthamiana leaves*. A 2,002 bp fragment upstream of the ATG start codon of *YUCCA8* fused with the firefly luciferase gene (LUC) was used as a reporter. Relative LUC activities were quantified as the ratios of LUC/REN enzyme activities and presented as means ± SD, $n = 6$. Asterisks represent statistically significant differences (**$P < 0.01$; n.s., not significant) determined by one-way ANOVA with Tukey's post hoc analysis.

enhance the transcriptional activation activity of PIF4 toward *IAA19*$_{pro}$:*LUC* or *IAA29*$_{pro}$:*LUC* when MYB112 and PIF4 were coexpressed in *N. benthamiana* leaves (Supplemental Fig. S5, C and D). Taken together, these results indicate that MYB112 physically interacts with PIF4 to enhance its transcriptional activation activity toward auxin-related genes.

PIF4 is epistatic to *MYB112* in regulating hypocotyl elongation

Furthermore, we investigated whether *MYB112* can genetically interact with *PIF4*. First, we generated *myb112-3 pif4-2* double mutants by crossing *myb112-3* into *pif4-2*. Both *myb112-3* and *pif4-2* single mutants showed short hypocotyls under different light conditions, and the hypocotyls of *pif4-2* were significantly shorter than those of *myb112-3*. The hypocotyls of the *myb112-3 pif4-2* double mutant were the same length as those of *pif4-2* (Fig. 4), suggesting that *MYB112* and *PIF4* act genetically in the same pathway. To test whether *PIF4* is epistatic to *MYB112*, we then crossed plants overexpressing *PIF4-Myc* (Dong et al. 2014) into *myb112-3*. The phenotypic results show that the hypocotyls of *PIF4-Myc myb112-3* are significantly longer than those of *myb112-3*, but slightly shorter than those of *PIF4-Myc* (Fig. 4), suggesting that the absence of *PIF4* contributes significantly to the short hypocotyl of *myb112-3*. Taken together, these data confirm that *MYB112* acts genetically upstream of *PIF4* to promote hypocotyl elongation in the light.

MYB112 suppresses the expression of *LUX* by direct binding to its promoter

Because MYB112 is an R2R3-MYB TF, we tested its biochemical activity in leaves of *N. benthamiana* using a transient expression assay. The full-length, N-terminal (1 to 170 aa), and C-terminal (171 to 243 aa) parts of MYB112 were each fused with the GAL4 BD, which could bind directly to the *GAL4* promoter (*GAL4*$_{pro}$) (Huai et al. 2018). As shown in Fig. 5A, full-length MYB112 significantly suppressed the expression of the *GAL4*$_{pro}$:*LUC* reporter. Moreover, MYB112-N did not affect the expression of *GAL4*$_{pro}$:*LUC*, whereas MYB112-C dramatically increased the expression of *GAL4*$_{pro}$:*LUC*. These results indicate that the full-length MYB112 protein has transcriptional repression activity, while its C-terminal region has strong transcriptional activation activity.

Because full-length MYB112 exhibits transcriptional repression activity (Fig. 5A) and indirectly promotes *PIF4* expression (Fig. 3A, Supplemental Fig. S6A), we speculate that target genes of MYB112 should be involved in repressing *PIF4* expression. Previous studies have shown that the EC ELF3-ELF4-LUX can repress the expression of *PIF4* under diurnal cycles. LUX can directly bind to the promoter of *PIF4* and recruit ELF3 and ELF4 together to repress *PIF4* expression (Nusinow et al. 2011). We examined the transcript levels of *ELF3*, *ELF4*, and *LUX* in seedlings of Col-0 and *myb112* mutants grown for 4 d under continuous white light (Fig. 5B). We found that the transcript levels of *ELF3* and *ELF4* showed no significant difference between Col-0 and *myb112* mutants, whereas the transcript levels of *LUX* were significantly upregulated in both *myb112-3* and *myb112-4* mutants compared with Col-0 (Fig. 5B). These results indicate that MYB112 can suppress the expression of *LUX* in the light.

We then used several experiments in vitro and in vivo to test whether *LUX* is a direct target gene of MYB112. Our Y1H assay showed that MYB112 was able to directly interact with the promoter of *LUX*, and the *LUX*$_{pro}$-N subfragment (−614 to −259 bp) was sufficient for this interaction in yeast cells (Fig. 5C). Because MYB112 was reported to bind to an 8 bp DNA fragment containing the core sequence (A/T/G)(A/C)CC(A/T)(A/G/T)(A/C)(T/C) (Lotkowska et al. 2015), the 50 bp subfragment (−308 to −259 bp upstream of ATG) in the *LUX* promoter, containing a potential MYB112 binding site, was used as a probe to perform an electrophoretic mobility shift assay (EMSA). His-TF-MYB112, but not His-TF protein (negative control), could bind to the promoter of *LUX* (Fig. 5D). Moreover, the binding could be abolished by introducing mutations into the potential binding site of the probe (Fig. 5D). The EMSA results suggest that MYB112 can bind to the specific motif in the promoter of *LUX* in vitro. To investigate whether MYB112 can bind to the promoter of *LUX* in vivo, we then performed chromatin immunoprecipitation (ChIP)-qPCR analysis. Our data showed that the B subfragment of the *LUX* promoter, which contained the core motif bound by MYB112 in vitro, was most enriched by YFP-MYB112 but not by YFP (Fig. 5E). Subsequent transient expression assays in *N. benthamiana* leaves show that MYB112 represses the expression of *LUX*$_{pro}$:*LUC* (Fig. 5F). Overall, our results confirm that MYB112 can repress the expression of *LUX* by directly binding to its promoter.

MYB112 genetically inhibits *LUX* to promote hypocotyl elongation

Considering the biochemical relationship between MYB112 and LUX, we moved to investigate the genetic relationship between *MYB112* and *LUX* in regulating hypocotyl elongation. First, we used the CRISPR/Cas9 system to generate a *lux* mutant, which was designated *lux-6* (Supplemental Fig. S7). Then, we generated a *myb112-3 lux-6* double mutant by crossing *myb112-3* into *lux-6*. Similar to previous reports (Helfer et al. 2011; Silva et al. 2020), *lux-6* exhibited longer hypocotyls than Col-0 under different light conditions. In addition, the hypocotyl lengths of *myb112-3 lux-6* were indistinguishable from those of *lux-6* (Fig. 6), indicating that *MYB112* acts upstream of *LUX* to promote hypocotyl elongation in the light.

MYB112 regulates *LUX* expression and PIF4 action in the afternoon under diurnal cycles

Our results confirm that MYB112 promotes hypocotyl elongation in the light (Fig. 1). Because the previous study has shown that high light stress (500 μmol m^{-2} s^{-1}) induces

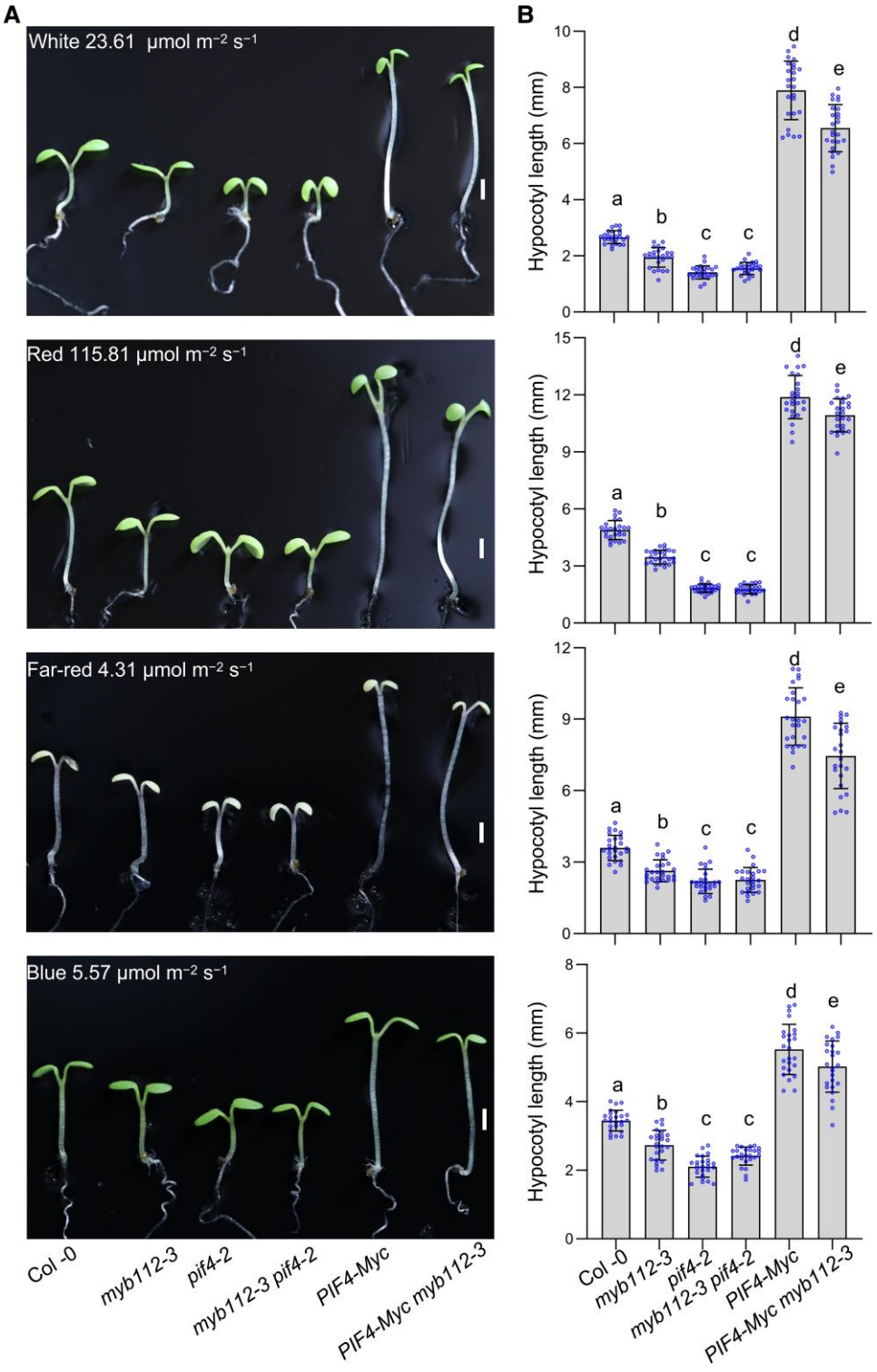

Figure 4. Genetic interaction between *MYB112* and *PIF4*. **A)** Hypocotyl phenotypes of Col-0, *myb112-3*, *pif4-2*, *myb112-3 pif4-2*, *PIF4-Myc*, and *PIF4-Myc myb112-3* grown for 4 d under continuous light conditions. Scale bars, 1 mm. **B)** Hypocotyl lengths of plant materials as indicated in **A)**. Data are presented as means ± SD, $n > 24$. Lowercase letters above the histogram represent statistically significant differences ($P < 0.05$) determined by one-way ANOVA with Tukey's post hoc analysis.

MYB112 expression (Lotkowska et al. 2015), we tested here whether MYB112 mRNA and protein levels are regulated by moderate light intensity. The RT-qPCR data showed that *MYB112* expression increased significantly when the seedlings were switched from dark to light (Fig. 7A), whereas it decreased gradually when the seedlings were switched

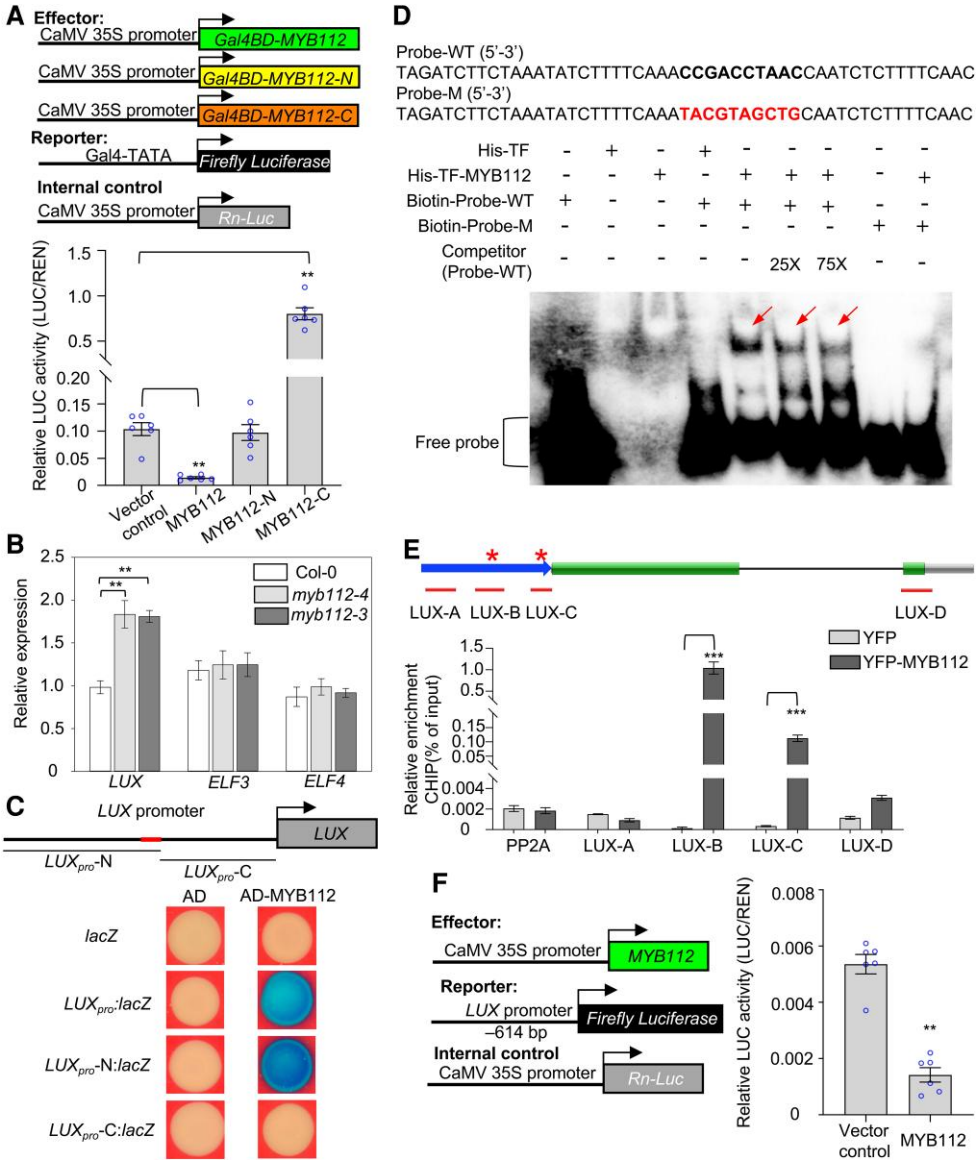

Figure 5. *LUX* acts as a target gene of MYB112. **A)** Transient expression assay showing the transcriptional activity of MYB112 in *N. benthamiana* leaves. The full-length, N-terminal (1 to 170 aa), and C-terminal (171 to 243 aa) parts of MYB112 were each fused with the GAL4 DNA-binding domain (Gal4BD). The *Gal4* promoter fused with the *LUC* gene was used as a reporter. Relative LUC activities were presented as means ± SD, $n = 6$. Asterisks represent statistically significant differences determined by Student's *t*-test (**$P < 0.01$). **B)** The relative expression of *LUX*, *ELF3*, and *ELF4* in Col-0 and *myb112* mutants. Relative transcript levels were normalized to *PP2A*. Error bars represent SD of three technical replicates. Asterisks represent statistically significant differences determined by Student's *t*-test (**$P < 0.01$). **C)** Yeast 1-hybrid assay showing that MYB112 bound directly to the *LUX* promoter. The CDS of *MYB112* was cloned into the pB42AD vector. The full-length fragment of the *LUX* promoter, its subfragments LUX_{pro}-N (−614 to −259 bp), and LUX_{pro}-C (−258 to −1 bp) were fused with *lacZ* reporter gene. AD, activation domain. The red line indicates the position of the probe used in **D)**. **D)** EMSA showing that MYB112 bound directly to the *LUX* promoter in vitro. A 50 bp subfragment of the *LUX* promoter, as indicated in **C)**, was used as a probe. Biotin-Probe-WT, the wild-type probe DNA labeled with biotin. Biotin-Probe-M, biotin-labeled probe with mutations at the potential MYB112 binding site (mutated nucleotides are shown in red). Competitor, biotin-unlabeled probes. 25× and 75× indicate the mole ratios of Competitor versus Biotin-Probe-WT. Red arrowheads indicate the DNA–protein complex. TF, trigger factor, a prokaryotic ribosome-associated chaperone protein. **E)** ChIP-qPCR assay showing that MYB112 associated with the *LUX* promoter in vivo. *YFP* and *YFP-MYB112* seedlings were used for the assay. The protein–chromatin complex was immunoprecipitated with GFP-trap beads. Values of ChIP were normalized to those of input DNA. *PP2A* was used as a negative control. Error bars represent SD of 3 technical replicates. The blue arrowhead in the gene body indicates the promoter, the green box indicates the exon regions, and the horizontal line indicates the intron regions. Red asterisks indicated the potential MYB112 binding sites. Asterisks above the histogram represent statistically significant differences (***$P < 0.001$) determined by one-way ANOVA with Tukey's post hoc analysis. **F)** Relative LUC expression driven by LUX_{pro} in *N. benthamiana* leaves. A 614 bp fragment upstream of the ATG start codon of *LUX*, fused with the *LUC* gene, was used as a reporter. Relative LUC activities are presented as means ± SD, $n = 6$. Asterisks above the histogram represent a statistically significant difference determined by Student's *t*-test (**$P < 0.01$).

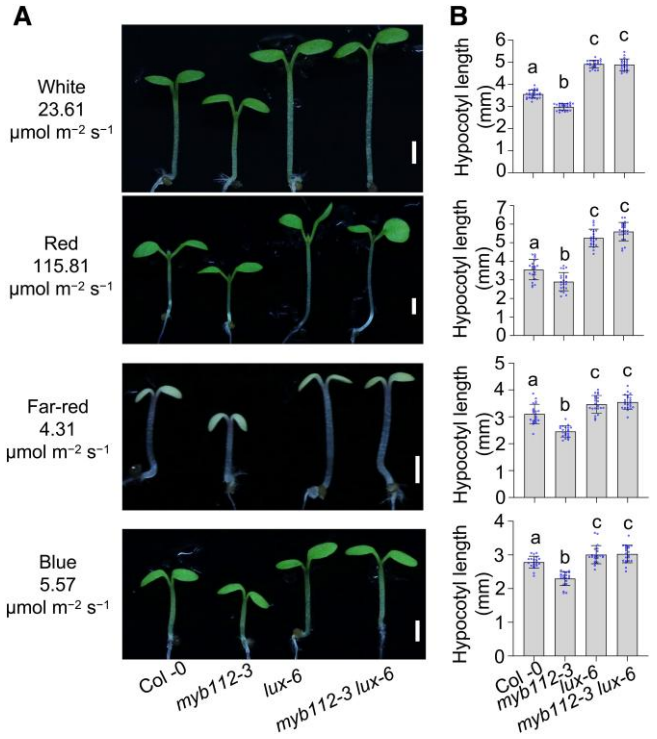

Figure 6. Genetic interaction between *MYB112* and *LUX*. **A)** Hypocotyl phenotypes of Col-0, *myb112-3*, *lux-6*, and *myb112-3 lux-6* grown for 4 d under continuous light conditions. Scale bars, 1 mm. **B)** Hypocotyl lengths of plant materials as indicated in **A)**. Data are presented as means ± SD, $n > 20$. Lowercase letters above the histogram represent statistically significant differences ($P < 0.05$) determined by one-way ANOVA with Tukey's post hoc analysis.

from light to dark (Supplemental Fig. S8A). Subsequently, the *YFP-MYB112* overexpression line driven by the 35S promoter was used to analyze the protein stability of MYB112. As shown in Fig. 7B, light significantly induced the accumulation of MYB112 protein, whereas MYB112 was dramatically degraded within 0.5 h when the seedlings were switched from light to dark (Supplemental Fig. S8B). The degradation of MYB112 in the dark could be inhibited by MG132 treatment, indicating that MYB112 is degraded in the dark via the 26S proteasome pathway (Supplemental Fig. S8C). These results suggest that light promotes the accumulation of both the mRNA and protein of MYB112. To further investigate whether *MYB112* is a clock-regulated gene, Col-0 seedlings were entrained for 6 d under 12 h light/12 h dark (12L/12D) cycles and then switched to continuous white light. Whole seedlings were harvested every 4 h and used for *MYB112* expression analysis by RT-qPCR. We found that *MYB112* expression did not exhibit a circadian rhythm (Supplemental Fig. S9), suggesting that *MYB112* expression is not regulated by the circadian clock.

LUX is an indispensable TF of the circadian clock; it targets EC to the *PIF4* promoter to repress its expression in the early evening (Nusinow et al. 2011). Since our results confirmed that MYB112 directly bound to the *LUX* promoter to inhibit its expression, we next asked whether MYB112 regulates the expression of *LUX* and *PIF4* under diurnal cycles. Col-0 and *myb112-3* were grown under 12L/12D cycles for 4 d, and then, whole seedlings were harvested every 4 h. Although the expression of *LUX* exhibited a diurnal rhythm in both Col-0 and *myb112-3*, the peak expression of *LUX* was significantly higher in *myb112-3* than in Col-0 at Zeitgeber time 8 (ZT8) in the afternoon (Fig. 7C). In contrast, the expression of *PIF4* was significantly lower in *myb112-3* than in Col-0 at ZT8 and ZT12 (Fig. 7D), consistent with the previous report that LUX suppressed *PIF4* expression under diurnal cycles (Nusinow et al. 2011; Ezer et al. 2017). These results show that MYB112 inhibits the expression of *LUX* and promotes the expression of *PIF4* mainly in the afternoon under 12L/12D cycles. To further investigate whether the decreased expression of *PIF4* in *myb112-3* is caused by the increased expression of *LUX* in *myb112-3*, we analyzed the transcript levels of *PIF4* at ZT8 and ZT12 in Col-0, *myb112-3*, *lux-6*, and *myb112-3 lux-6* grown under 12L/12D cycles. Expression of *PIF4* was slightly higher in *lux-6* than in Col-0 at ZT8, and this difference in expression became even more pronounced at ZT12 (Fig. 7E). The absence of *LUX* in *myb112-3* significantly rescued the impaired expression of *PIF4* in *myb112-3* at ZT8 (Fig. 7E). Moreover, *PIF4* expression in *myb112-3 lux-6* was significantly higher than that in *myb112-3* and equal to that in *lux-6* at ZT12 (Fig. 7E). These results confirm that MYB112 promotes *PIF4* expression by suppressing *LUX* expression in the afternoon under diurnal cycles. Genetic evidence showed that the hypocotyls of *myb112-3* were significantly shorter than those of Col-0 under different diurnal cycles (Fig. 7F), suggesting that MYB112 promotes hypocotyl elongation under diurnal cycles. Mutation of *LUX* in *myb112-3* resulted in hypocotyl elongation, and the hypocotyls of *myb112-3 lux-6* were as long as those of the *lux-6* single mutant under 12L/12D or 8L/16D cycles (Fig. 7F), suggesting that *LUX* also acts downstream of *MYB112* in regulating hypocotyl elongation under different diurnal cycles.

Since we have shown that MYB112 physically interacts with PIF4 to enhance its transcriptional activation activity (Fig. 3, Supplemental Fig. S5), we next sought to determine when they interact to promote the expression of PIF4 target genes under diurnal cycles. First, $MYB112_{pro}$:*MYB112-GFP*/*myb112-3* and $MYB112_{pro}$:*MYB112-GFP*/*myb112-4* transgenic plants were generated (Supplemental Fig. S10), and they were able to rescue the hypocotyl elongation defect of *myb112-3* and *myb112-4*, respectively (Supplemental Fig. S10, B and C), indicating that the MYB112-GFP proteins produced in these 2 transgenic plants are biologically functional. The $MYB112_{pro}$:*MYB112-GFP*/*myb112-3* #6 line was used to analyze the temporal accumulation pattern of MYB112 protein under 12L/12D cycles. As shown in Fig. 7G, MYB112-GFP proteins accumulated mainly during daytime (ZT4 and ZT8). Using the PIF4 antibody, the temporal accumulation pattern of endogenous PIF4 proteins under diurnal cycles was analyzed in Col-0. Endogenous PIF4 proteins also accumulated

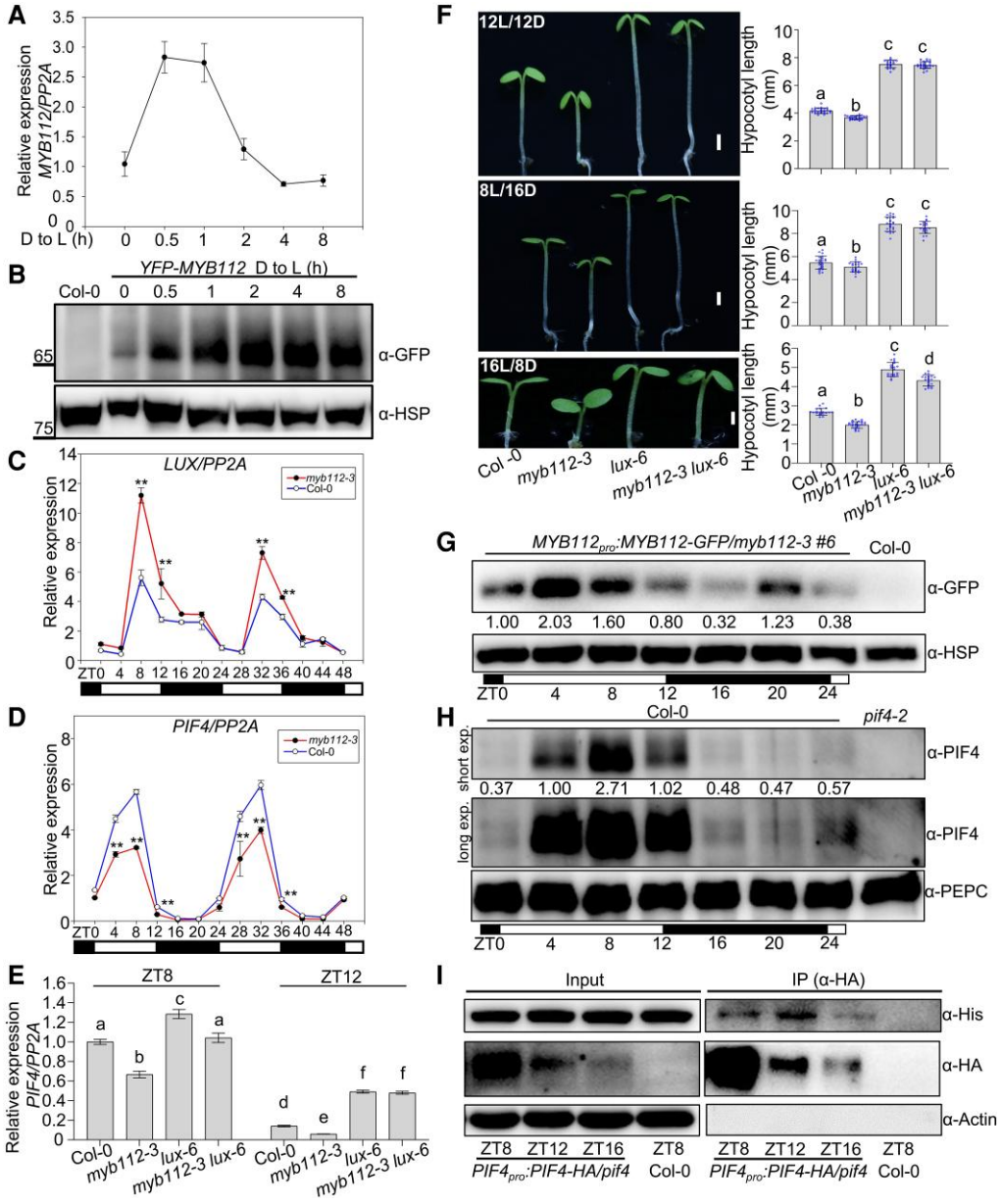

Figure 7. MYB112 regulates *LUX* expression and PIF4 action in the afternoon under diurnal cycles. **A)** The relative expression of *MYB112* when seedlings were switched from dark to light. Relative transcript levels were normalized to *PP2A*. Error bars represent SD of 3 technical replicates. D, darkness; L, continuous white light (55.07 μmol m^{-2} s^{-1}). **B)** The change in YFP-MYB112 protein levels when seedlings were switched from dark to light for the indicated period. *YFP-MYB112*, transgenic seedlings overexpressing YFP-tagged MYB112; D, darkness; L, continuous white light (55.07 μmol m^{-2} s^{-1}). The relative expression of *LUX* **C)** and *PIF4* **D)** in Col-0 and *myb112-3* grown under 12 h light/12 h dark (12L/12D) cycles. Relative transcript levels were normalized to *PP2A*. Error bars represent SD of 3 technical replicates. ZT, zeitgeber. The rectangles under the graphs represent the light conditions during harvest: black, light off; white, light on. Relative transcript levels were normalized to *PP2A* transcript levels. Asterisks represent statistically significant differences determined by Student's *t*-test (**$P < 0.01$). **E)** The relative expression of *PIF4* at ZT8 and ZT12 in Col-0, *myb112-3*, *lux-6*, and *myb112-3 lux-6* grown under 12L/12D cycles. Relative transcript levels were normalized to *PP2A* transcript levels. Error bars represent SD of 3 technical replicates. Lowercase letters above the histogram represent statistically significant differences (**$P < 0.01$) determined by one-way ANOVA with Tukey's post hoc analysis. **F)** Hypocotyl phenotypes and lengths of Col-0, *myb112-3*, *lux-6*, and *myb112-3 lux-6* grown under 12L/12D, 8L/16D, or 16L/8D cycles, respectively. Data are presented as means ± SD, $n > 16$. Lowercase letters above the histogram represent statistically significant differences ($P < 0.05$) determined by one-way ANOVA with Tukey's post hoc analysis. Temporal accumulation patterns of MYB112 **G)** and PIF4 **H)** under diurnal cycles. Seedlings grown for 6 d under 12L/12D cycles were harvested every 4 h. HSP **G)** and PEPC **H)** were each used as loading controls. Short exp., short exposure; Long exp., long exposure. Numbers below the lanes indicate relative band intensities of MYB112-GFP **G)** or PIF4 **H)**. **I)** Semi–in vivo Co-IP assay showing the time course of interaction between MYB112 and PIF4. Six-day-old *PIF4pro:PIF4-HA/pif4* seedlings grown under 12L/12D cycles were harvested from ZT8 to ZT16. PIF4-HA was immunoprecipitated with anti-HA nanobody beads. Actin was used as a loading control.

significantly during the day and peaked at ZT8 (Fig. 7H), which was similar to previous reports (Bernardo-García et al. 2014; Gao et al. 2022). These results indicate that the coaccumulation of MYB112 and PIF4 proteins begins in the morning, and the expression of both proteins subsequently overlaps until the end of the day.

Next, we performed a semi–in vivo Co-IP assay using His-TF-MYB112 protein and the previously reported *PIF4*$_{pro}$:*PIF4-HA*/*pif4* seedlings (Zhang et al. 2017). Because endogenous PIF4 proteins peaked at ZT8 and then decreased (Fig. 7H), *PIF4*$_{pro}$:*PIF4-HA*/*pif4* seedlings harvested from ZT8 to ZT16 were used for the Co-IP. The same amount of His-TF-MYB112 was incubated with total extracts from *PIF4*$_{pro}$:*PIF4-HA*/*pif4* seedlings harvested at different timepoints, respectively. PIF4-HA proteins could coimmunoprecipitate more His-TF-MYB112 at ZT8 and 12 than at ZT16 (Fig. 7I). All in all, this suggests that MYB112 interacts with PIF4 at least in the afternoon under 12L/12D cycles.

Discussion

Numerous studies have confirmed that light is a crucial cue determining photomorphogenesis of Arabidopsis seedlings (Vierstra and Quail 1983; Sharrock and Quail 1989; Deng et al. 1991; Lin et al. 1995; Osterlund et al. 2000; Leivar et al. 2008b; Rizzini et al. 2011; Christie et al. 2012; Liu et al. 2020). The endogenous circadian clock adjusts seedling photomorphogenesis to the day–night cycle, thereby optimizing the environmental adaptation of Arabidopsis (Nozue et al. 2007; Nusinow et al. 2011; Su et al. 2021; Xu et al. 2022). PIF4 acts downstream of both light and circadian clock signals to promote hypocotyl elongation (Huq and Quail 2002; Nozue et al. 2007; Leivar et al. 2008b; Nusinow et al. 2011). Transcription of *PIF4* is inhibited by EC of circadian oscillators mainly in the early evening under diurnal cycles. At the end of the night, attenuated inhibition of *PIF4* transcription by EC, combined with protein accumulation of PIF4, dramatically promotes hypocotyl elongation (Nusinow et al. 2011). LUX targets EC to the promoter of *PIF4* to repress its expression. The *lux* single mutant shows accelerated hypocotyl elongation under diurnal cycles, indicating an indispensable role of LUX in the function of EC in regulating photoperiodic hypocotyl growth (Helfer et al. 2011; Nusinow et al. 2011). It has been reported that ELONGATED HYPOCOTYL 5 (HY5), the key TF promoting photomorphogenesis, binds directly to the *LUX* promoter and represses its transcription specifically under blue light (Hajdu et al. 2018). However, the biological function of HY5-mediated regulation of *LUX* transcription is still unknown. Further studies are needed to uncover the mechanism of light-controlled regulation of *LUX* transcription. In this study, we demonstrated that light-regulated MYB112 could bind directly to the *LUX* promoter to repress its expression. The light signal induced both transcript and protein accumulation of MYB112. On the one hand, MYB112 bound directly to the *LUX* promoter to repress its expression in the afternoon under diurnal cycles, relieving LUX-inhibited expression of *PIF4*. On the other hand, MYB112 physically interacted with PIF4 at least in the afternoon to enhance the ability of PIF4 to activate the expression of auxin-related genes. Thus, the enhanced transcript accumulation and transcriptional activation activity of PIF4 by MYB112 additively promoted the expression of auxin-related genes, thereby increasing auxin synthesis and signaling and fine-tuning hypocotyl growth under diurnal cycles (Fig. 8).

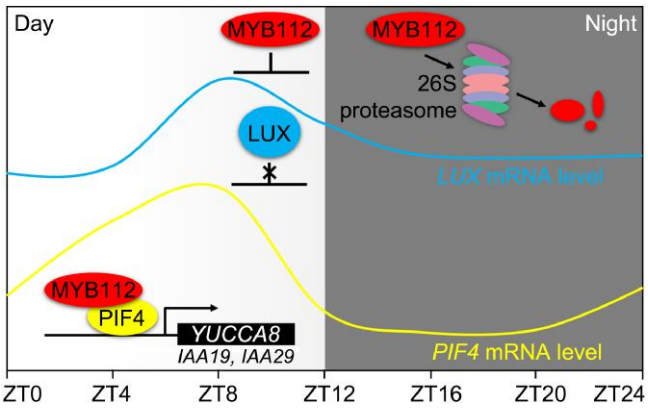

Figure 8. Proposed working model showing how MYB112 promotes hypocotyl elongation under diurnal conditions.

MYB112 is a member of the R2R3-MYB TF family, which contains 126 members in Arabidopsis (Millard et al. 2019). Numerous R2R3-MYB TFs have been found to be involved in regulating plant-specific processes, including secondary metabolism and response to biotic and abiotic stresses (Mengiste et al. 2003; Stracke et al. 2007; Dubos et al. 2010). Among these, only 4 members, i.e. MYB18/LONG AFTER FAR-RED LIGHT 1 (LAF1), MYB30, MYB38, and MYB61, have been shown to be involved in regulating seedling photomorphogenesis (Ballesteros et al. 2001; Newman et al. 2004; Hong et al. 2008; Yan et al. 2020). Nonetheless, whether R2R3-MYB TFs are involved in connecting the light and clock signaling pathways during seedling photomorphogenesis remains completely unknown. In addition, although a previous study has shown that MYB112 is involved in anthocyanin biosynthesis under abiotic stress, the distinct biological function of MYB112 remains unreported (Lotkowska et al. 2015). In this study, mutation of *MYB112* impaired hypocotyl elongation of seedlings under either constant light or diurnal conditions (Supplemental Fig. S1; Figs. 1 and 7F). In contrast, overexpression of *MYB112* in vivo promoted hypocotyl elongation in the light (Supplemental Fig. S3; Fig. 1). We further dissected the molecular mechanism underlying MYB112-induced hypocotyl elongation (Fig. 8). All these results shed light on the molecular function of MYB112 in connecting light and clock signaling pathways and on the biological function of MYB112 in regulating hypocotyl elongation under diurnal cycles. It will be of great interest to test the potential roles of other R2R3-MYB TFs in regulating photomorphogenesis.

Our results showed that MYB112 physically interacts with PIF4 to enhance the expression of PIF4 target genes *IAA19*, *IAA29*, and *YUCCA8* (Fig. 3; Supplemental Fig. S5). However, the mechanism of MYB112-regulated transcriptional activation activity of PIF4 needs further investigation. PIF4 is a well-known TF that plays a central role in seedling photomorphogenesis, and the regulatory mechanisms for PIF4 activity have been extensively studied. Several factors regulate PIF4 activity by affecting its ability to bind to target genes. For example, activated phyB can not only trigger PIF4 degradation but also sequestrate PIF4 to inhibit its DNA-binding ability (Park et al. 2018). In contrast, TCP15 physically interacts with PIF4 to enhance PIF4's association with DNA (Ferrero et al. 2019). Therefore, it is possible that the interaction of MYB112 and PIF4 may increase the affinity of PIF4 for the promoters of its target genes. Interestingly, although full-length MYB112 exhibited transcriptional repression activity, the C-terminus of MYB112 showed significant transcriptional activation activity (Fig. 5A). Similar to MYB112, most R2R3-MYB TFs harbor MYB BD in the N-terminus and intrinsically disordered regions (IDRs) in the C-terminus (Millard et al. 2019). Several lines of evidence have linked IDRs to the activation activity of R2R3-MYB TFs (Ballesteros et al. 2001; Zhang et al. 2009; Lee et al. 2016; Stracke et al. 2017). It is possible that the interaction between the N-terminus of MYB112 and PIF4 releases the activation activity of the C-terminus of MYB112, thereby coordinating PIF4 to increase gene expression. This should be investigated in a future study.

Our results showed that MYB112 transcript and protein accumulated during the dark-to-light transition (Fig. 7, A and B) and that MYB112 protein was degraded in the dark via the 26S proteasome pathway (Supplemental Fig. S8, B and C). Nonetheless, the component required for MYB112 degradation in the dark remains unknown. Phylogenic analysis shows that MYB112 belongs to subgroup 20 of the R2R3-MYB TF family. Subgroup 20 contains 5 other members. Among them, MYB108, also known as BOTRYTIS-SUSCEPTIBLE1 (BOS1) (Mengiste et al. 2003), is described as a potential substrate of the E3 ligase Botrytis-Susceptible1 Interactor (BOI) (Luo et al. 2010). Compared with Col-0, transgenic plants overexpressing BOI exhibit significantly shorter hypocotyls (Park et al. 2013), similar to those of *myb112* mutants. Further studies should be conducted to test the potential interaction between MYB112 and BOI.

To summarize, our study reveals the biological function and molecular mechanism of MYB112 in connecting light and clock signaling pathways to regulate hypocotyl elongation. It also sheds light on the function of R2R3-MYB TFs in connecting light and clock signaling pathways to regulate seedling photomorphogenesis.

Methods

Plant materials, growth conditions, phenotypic analyses, and antibodies

The accession of all wild-type *A. thaliana* plants used in this study was Col-0. Seeds were first surface sterilized with 10% (*v*/*v*) sodium hypochlorite solution for 20 min and then grown on Murashige and Skoog (MS) medium, pH 5.7, supplemented with 1% (*w*/*v*) sucrose (Sangon Biotech) and 0.8% (*w*/*v*) agar (Sigma-Aldrich), followed by stratification at 4 °C in the dark for 48 h. Seeds were then germinated and grown at 22 °C in the light chamber (Percival) under different light conditions, such as continuous darkness, white light (23.61 μmol m^{-2} s^{-1}), red light (115.81 μmol m^{-2} s^{-1}), far-red light (4.31 μmol m^{-2} s^{-1}), or blue light (5.57 μmol m^{-2} s^{-1}) conditions, depending on the requirements of the experiments. Four-day-old seedlings were photographed with a digital single-lens reflex camera (EOS 80D, Canon), and hypocotyl lengths were measured using ImageJ software.

The *A. thaliana pif4-2* mutant used in this study was reported previously (Leivar et al. 2008a). *myb112* mutants were generated using the CRISPR/Cas9 system (Wang et al. 2015). Two target sites in the first exon of *MYB112* were selected (Supplemental Fig. S1A) using the web tool CRISPR-P (http://crispr.hzau.edu.cn/CRISPR/) (Lei et al. 2014). *Agrobacterium tumefaciens* strain GV3101 carrying the CRISPR/Cas9 expression vectors was used to transform Col-0 plants by the floral dip method (Clough and Bent 1998). We selected primary transformants with MS medium containing 50 mg/L hygromycin and genotyped these plants by PCR amplification and sequencing analysis with specific primers for *MYB112* (Supplemental Data Set 2). We identified 2 types of mutations (M1/47 bp deletion and M2/59 bp deletion) that were homozygous for null alleles of *MYB112* induced by CRISPR/Cas9, which were designated as *myb112-3* and *myb112-4*, respectively (Supplemental Fig. S1A). Subsequently, the corresponding "transgene-free" homozygous *myb112* mutants were screened in their progeny using MS medium containing 50 mg/L hygromycin and PCR amplification with sequencing analysis. Using the same principle, 2 target sites in the first exon of *LUX* were selected (Supplemental Fig. S7A). We identified 1 type of mutation (32 bp deletion) that was homozygous for the null allele of *LUX* induced by CRISPR/Cas9, which was designated as *lux-6* (Supplemental Fig. S7A).

To generate transgenic plants overexpressing *MYB112*, we cloned the full-length coding sequence (CDS) of *MYB112* into the pDONR-223 vector (Invitrogen) using Gateway BP Clonase™ II Enzyme Mix (Invitrogen) and verified the construct by sequencing. We further introduced the CDS-containing vector into the pEarleyGate 104 (N-terminal eYFP tag) vector (Earley et al. 2006) using Gateway LR Clonase™ II Enzyme Mix (Invitrogen) to generate the plant binary construct pEarleyGate-YFP-*MYB112*. GV3101 carrying the construct was used to transform Col-0 plants. Homozygous transgenic lines were screened with MS medium containing 20 mg/L glufosinate ammonium. Overexpression of *MYB112* in the transgenic lines was then detected by RT-qPCR and immunoblot with anti-GFP antibody. Based on the results of RT-qPCR and immunoblot, we selected 2 lines (*YFP-MYB112 #2* and *#3*) for further study (Supplemental Fig. S3). To generate $MYB112_{pro}$:*MYB112-GFP*/*myb112-3* and

MYB112$_{pro}$:*MYB112-GFP*/*myb112-4* transgenic plants, the *MYB112* promoter (2,000 bp upstream of the ATG start codon), the full-length CDS of *MYB112*, and *GFP* were amplified by PCR and integrated into the pCambia1300 vector. The construct was then transferred into the *myb112-3* or *myb112-4* mutant via GV3101-mediated transformation. Homozygous transgenic lines were screened with MS medium containing 50 mg/L hygromycin and immunoblot with anti-GFP antibody. All primers used in this study are listed in Supplemental Data Set 2.

All commercial antibodies used in this study are listed below: anti-PIF4 (1:2,000 [*v*/*v*], catalog no. R2534-4; Abicode), anti-His (1:1,000 [*v*/*v*], catalog no. H1029; Sigma-Aldrich), anti-GST (1:1,000 [*v*/*v*], catalog no. AE006; Abclonal), anti-GFP (1:5,000 [*v*/*v*], catalog no. M20004; Abmart), anti-Myc (1:2,000 [*v*/*v*], catalog no. C3956; Sigma-Aldrich), anti-HA (1:5,000 [*v*/*v*], catalog no. H9658; Sigma-Aldrich), anti-Histone 3 (1:5,000 [*v*/*v*], catalog no. H0164; Sigma-Aldrich), anti-HSP (1:5,000 [*v*/*v*], catalog no. AbM51099-31-PU; Beijing Protein Innovation), anti-Actin (1:2,000 [*v*/*v*], catalog no. AC009; Abclonal), and anti-PEPC (1:2,000 [*v*/*v*], catalog no. AS09 458; Agrisera).

RNA-seq analysis

Col-0 and *myb112-4* mutant seedlings were grown under continuous white light (23.61 μmol m^{-2} s^{-1}) conditions for 4 d before sampling. Total RNA was extracted using an E.Z.N.A. Plant RNA Kit (Omega Bio-tek). RNA-seq libraries were prepared, and their qualities were determined using an Agilent 2100 Bioanalyzer from Novogene Bioinformatics Technology Co. Ltd. and then sequenced using the Illumina method. The raw reads were cleaned and mapped to the Arabidopsis TAIR10 genome. Differential gene expression analysis was performed using the edgeR likelihood ratio test (Robinson et al. 2009). Genes with false discovery rate (FDR) < 0.05 were selected for subsequent analysis.

Quantitative real-time PCR

Total RNA was isolated from Arabidopsis seedlings using an E.Z.N.A. Plant RNA Kit (Omega Bio-tek). For reverse transcription, 1 μg of total RNA was used as a template to generate first-strand cDNA using the All-In-One 5× RT Master Mix (Applied Biological Materials). RT-qPCR was performed using the ABI QuantStudio™ 6 Flex Real-Time PCR System following the manufacturer's instruction. The relative expression level of genes was analyzed using the $2^{-\Delta\Delta Ct}$ method, with the value of *PP2A* expression serving as an internal control.

Yeast 1-hybrid and yeast 2-hybrid assays

The N-terminal (1 to 510 bp), C-terminal (511 to 732 bp), and full-length CDS of *MYB112* were amplified by PCR (Supplemental Data Set 2) and cloned into the pLexA and pB42AD vectors (Clontech) to generate pLexA-*MYB112-N*, pLexA-*MYB112-C*, pLexA-*MYB112*, and pB42AD-*MYB112* constructs, respectively. The full-length CDS of *PIF4* was amplified by PCR (Supplemental Data Set 2) and cloned into the pB42AD vector to generate the pB42AD-*PIF4* vector. The promoters of *PIF4* (−2428 to −89 bp, −2428 to −1108 bp, −1145 to −89 bp, and −1145 to −456 bp) were amplified by PCR (Supplemental Data Set 2) and cloned into the pLacZ2U vector (Clontech). The promoter of *YUCCA8* (2,002 bp upstream of the ATG start codon) and its subfragment containing G-box (−650 to −451 bp), and the promoter of *LUX* (614 bp upstream of the ATG start codon) and its subfragments *LUX*$_{pro}$-N (−614 to −259 bp) and *LUX*$_{pro}$-C (−258 to −1 bp) were amplified by PCR (Supplemental Data Set 2) and cloned into the reporter plasmid pLacZ2u.

For the Y1H assay, various pB42AD and pLacZ2u recombination constructs were cotransformed into yeast strain EGY48. Transformants were grown on a minimal synthetic defined (SD) base supplemented with the −Ura/−Trp dropout (DO) mix and X-gal (5-bromo-4-chloro-3-indolyl-β-D-galactopyranoside) for blue color development. For the Y2H assay, various pB42AD and pLexA recombination constructs were cotransformed into yeast strain EGY48 containing p8op-LacZ vector. Transformants were grown on SD/-His-Trp-Ura medium with X-gal for blue color development. β-Galactosidase activity was quantified by liquid culture assays using o-nitrophenyl-β-D-galactopyranoside (ONPG, Amresco) as the substrate, and Miller Units were calculated according to the Yeast Protocols Handbook (Clontech).

LCI assay

The LCI assay was performed as previously described (Chen et al. 2008). The full-length CDS of *MYB112* and *PIF4* were amplified by PCR (Supplemental Data Set 2) and cloned into the *cLUC* and *nLUC* vectors, respectively (Chen et al. 2008). These vectors were individually transformed into *A. tumefaciens* strain GV3101 and then infiltrated into fully expanded young leaves of *N. benthamiana* using a needleless syringe. After infiltration, plants were grown for 3 d under 16 h light/8 h dark conditions. The Night SHADE LB 985 (Berthold Technologies) system was used to capture the luciferase signal.

Purification of recombinant proteins

The full-length CDS of *MYB112* was amplified by PCR (Supplemental Data Set 2) and cloned into the pGEX-4T-1 and pCold-TF vectors. The full-length CDS of *PIF4* was amplified by PCR (Supplemental Data Set 2) and cloned into the pCold-TF vector. These vectors were verified by sequencing and then transformed into *Escherichia coli* strain BL21. To induce the expression of GST-MYB112, His-TF-MYB112, and His-TF-PIF4 proteins, these bacterial solutions were treated with 0.8 mM IPTG (isopropyl β-D-thiogalactoside) and incubated overnight at 16 °C. Bacterial cells were collected by centrifugation at 3783 × *g* for 5 min at 4 °C. GST-tagged proteins were purified with Glutathione Sepharose™ 4B (GE Healthcare), and TF-tagged protein was purified with Ni-NTA agarose (QIAGEN). Following the same principle,

GST and His-TF proteins were purified and used as the control group for further experiments.

In vitro pull-down assay

For the in vitro pull-down assay, 10 μg GST-MYB112 and 10 μg His-TF-PIF4 were incubated in 1 mL binding buffer (20 mM Tris-HCl, pH 8.0, 200 mM NaCl, 10% [*v*/*v*] glycerol, and 1 mM PMSF) at 4 °C for 2 h. 20 μL Glutathione Sepharose™ 4B (GE Healthcare) was added to the binding buffer and then incubated for an additional 2 h. The beads were then washed 5 times with the binding buffer, and the proteins were eluted in 1× SDS loading buffer at 100 °C for 10 min. The eluted proteins were separated on 10% (*w*/*v*) SDS-PAGE gels and detected by immunoblotting using anti-His and anti-GST antibodies.

Co-IP assays

Co-IP experiments were performed as previously described with minor modifications (Li et al. 2020). Briefly, about 0.6 g seedlings grown for 6 d under continuous white light were harvested, ground into powder, and added to Co-IP lysis buffer containing 50 mM Tris-HCl (pH 7.5), 150 mM NaCl, 1 mM EDTA, 10% (*v*/*v*) glycerol, 0.1% (*v*/*v*) Tween-20, 1 mM PMSF, and 1× protease inhibitor cocktail (Roche). Total proteins were extracted by centrifugation at 12,000× *g* for 10 min at 4 °C, and protein concentrations were determined using the Bradford quantification kit. Two milligrams total proteins were incubated with 15 μL GFP-Trap beads (catalog no. gta-20; ChromoTek) for 3 h at 4 °C. After incubation, the beads were washed 3 times with 500 μL washing buffer (20 mM Tris-HCl [pH 8.0], 150 mM NaCl, 1 mM EDTA, 10% (*v*/*v*) glycerol, and 1× protease inhibitor cocktail) at 4 °C. Then, the immunoprecipitated proteins were eluted with 1× SDS loading buffer and detected by immunoblotting using anti-GFP, anti-Myc, and anti-Actin antibodies.

For semi–in vivo Co-IP, Col-0 and *PIF4*$_{pro}$*:PIF4-HA/pif4* seedlings grown under 12L/12D cycles were harvested, ground to powder in liquid nitrogen, and added into lysis buffer (25 mM Tris-HCl [pH 7.5], 150 mM NaCl, 1 mM EDTA, 10% [*v*/*v*] glycerol, 0.1% [*v*/*v*] Tween-20, 2× protease inhibitor cocktail). The lysates were sonicated to disrupt the nuclei. 500 μg total proteins were incubated with 8 μg His-TF-MYB112 protein in 0.6 mL lysis buffer for 2 h at 4 °C, and then, 10 μL anti-HA nanobody beads (catalog no. KTSM1305; AlpalifeBio) were added and incubated with the mixture for another 1.5 h at 4 °C. Beads were then washed 3 times with 50 column volumes of washing buffer (25 mM Tris-Cl [pH 7.5], 150 mM NaCl, 1 mM EDTA, 10% [*v*/*v*] glycerol, 0.02% [*v*/*v*] Tween-20, 1× protease inhibitor cocktail). Proteins were eluted with 1× SDS loading buffer and analyzed by immunoblotting with anti-His, anti-HA, and anti-Actin antibodies.

Transient dual-luciferase assays

The full-length CDS of *MYB112* and *PIF4* were amplified by PCR (Supplemental Data Set 2) and cloned into the pGreenII 62-SK vector (Hellens et al. 2005) to generate pGreenII 62-SK-*MYB112* and pGreenII 62-SK-*PIF4* constructs. The promoters of *LUX* (614 bp upstream of ATG), *IAA19* (1,755 bp upstream of ATG), *IAA29* (1,888 bp upstream of ATG), and *YUCCA8* (2,002 bp upstream of ATG) were amplified by PCR (Supplemental Data Set 2) and cloned into the reporter vector pGreenII 0800-LUC (Hellens et al. 2005). These vectors were individually transformed into *A. tumefaciens* strain GV3101 and then infiltrated into fully expanded young leaves of *N. benthamiana* using a needleless syringe. After infiltration, plants were grown for 3 d under 16 h light/8 h dark conditions. Luminescent signals of LUC and RENILLA (REN) were detected using the Dual-Luciferase Reporter Assay System (Promega). The ratio of LUC/REN was calculated as the expression levels of *LUC*.

For the MYB112 transcriptional activity assay, the N-terminal (1 to 510 bp), C-terminal (511 to 732 bp), and full-length CDS of *MYB112* were amplified by PCR (Supplemental Data Set 2) and cloned into the effector vector pEAQ-GAL4BD to generate the pEAQ-GAL4BD-*MYB112-N*, pEAQ-GAL4BD-*MYB112-C*, and pEAQ-GAL4BD-*MYB112* constructs. *GAL4*$_{pro}$*:LUC* was used as the reporter. These vectors were individually transformed into *A. tumefaciens* strain GV3101 and then infiltrated into fully expanded young leaves of *N. benthamiana* using a needleless syringe. After infiltration, plants were grown for 3 d under 16 h light/8 h dark conditions. Luminescent signals of LUC and REN were detected using the Dual-Luciferase Reporter Assay System (Promega). The ratio of LUC/REN was calculated as the expression levels of *LUC*.

EMSA

The 50 bp subfragment of *LUX* promoter (−308 to −259 bp), which contained a potential MYB112 binding site, was used as a probe to perform EMSA. The sequences of the wild-type probe (Probe-WT) and the mutant probe (Probe-M, with mutations at the potential binding site) are listed in Supplemental Data Set 2. The double-stranded probes were labeled with biotin using the EMSA Probe Biotin Labeling Kit (Beyotime Biotech). EMSA was performed as previously described (Hellman and Fried 2007). Incubation of proteins and probes was performed following the instruction of the LightShift EMSA Optimization and Control Kit (Thermo Scientific). Briefly, 1.5 μg His-TF-MYB112 protein and 50 fmol biotin-labeled probe were incubated for 30 min at room temperature in 20 μL binding buffer containing 1× binding buffer, 0.05 μg/μL Poly (dI-dC), 2.5% (*v*/*v*) glycerol, 5 mM $MgCl_2$, and 0.05% (*v*/*v*) Nonidet P-40. The DNA–protein complex was separated on 5% (*w*/*v*) native polyacrylamide gels containing 2.5% (*v*/*v*) glycerol. Electrophoresis was carried out in an ice-water bath to avoid high temperature of the gels. Probes were then electroblotted to Hybond N^+ (Millipore) nylon membranes in an ice-water bath and detected following the instructions of the LightShift Chemiluminescent EMSA Kit (Thermo Scientific).

ChIP-qPCR

Seedlings overexpressing *YFP-MYB112* or *YFP* were grown under continuous white light (99.07 μmol m^{-2} s^{-1}) for 5 d and harvested for ChIP assays. First, 2 g seedlings were fixed in 37 mL 1% (*v*/*v*) formaldehyde under vacuum for 15 min, and then, 2.5 mL 2 M glycine was added to stop the reaction. The tissue was rinsed 3 times with 35 mL ddH_2O to remove all the formaldehyde. After that, the ddH_2O was removed as thoroughly as possible using filter papers. The fixed tissue was ground into powder and added to 30 mL extraction buffer 1 containing 0.4 M sucrose, 10 mM Tris-HCl (pH 8.0), 10 mM $MgCl_2$, 5 mM β-ME (β-mercaptoethanol), 1× protease inhibitor cocktail (Roche), and 0.1 mM PMSF. The homogeneous solution was filtered through a 2-layer Miracloth (Millipore) into a fresh 50 mL tube and then centrifuged at 3,000×*g* for 20 min at 4 °C. The pellet was resuspended in 1 mL extraction buffer 2 containing 0.25 M sucrose, 10 mM Tris-HCl (pH 8.0), 10 mM $MgCl_2$, 5 mM β-ME, 1% (*v*/*v*) Triton X-100, 1× protease inhibitor cocktail, and 0.1 mM PMSF. The solution was centrifuged at 12,000×*g* at 4 °C for 10 min. The pellet was resuspended in 500 μL extraction buffer 3 containing 1.70 M sucrose, 10 mM Tris-HCl (pH 8.0), 2 mM $MgCl_2$, 5 mM β-ME, 0.15% (*v*/*v*) Triton X-100, 1× protease inhibitor cocktail, and 0.1 mM PMSF. The solution was centrifuged at 15,000×*g* at 4 °C for 1 h. The chromatin solution was sonicated in nuclei lysis buffer (50 mM Tris-HCl [pH 8.0], 10 mM EDTA, 1% (*w*/*v*) SDS, and 0.1 mM PMSF) at 4 °C to generate 250 to 500 bp fragments. Approximately 10% (*v*/*v*) of the sonicated solution was used as input DNA control. The protein–chromatin complexes were immunoprecipitated with GFP-Trap beads at 4 °C overnight. The crosslinked status of the chromatin was reversed, and the enrichments of 4 regions in the *LUX* promoter (*LUX*-A, B, C, and D) were analyzed by RT-qPCR. Primers used for ChIP assays are listed in Supplemental Data Set 2.

Quantification and statistical analysis

Band intensities of immunoblot results were quantified using ImageJ software. Statistical analyses were performed using GraphPad Prism 8 software. The summary of statistical analyses is presented in Supplemental Data Set 3.

Accession numbers

Sequence data from this article can be found in the Arabidopsis TAIR database (www.arabidopsis.org) under the following accession numbers: *MYB112* (At1g48000), *PIF1* (At2g20180), *PIF3* (At1g09530), *PIF4* (At2g43010), *PIF5* (At3g59060), *PIF7* (At5g61270), *LUX* (At3g46640), *ELF3* (At2g25930), *ELF4* (At2g40080), *YUCCA8* (At4g28720), *IAA19* (At3g15540), *IAA29* (At4g32280), and *PP2A* (At1g69960). The raw RNA-seq data for this study were deposited in the NCBI Sequence Read Archive under BioProject ID PRJNA963228 with accession number SRP435210.

Acknowledgments

We thank Li Yang (China Agricultural University) for her valuable suggestions on the manuscript. We thank Jie Dong (Zhejiang University) for his critical suggestions on revising the manuscript. We are grateful to Ove Nilsson (Swedish University of Agricultural Sciences) for providing the *PIF4*$_{pro}$:*PIF4-HA*/*pif4* transgenic line. This work was supported by the National Natural Science Foundation of China (Grant Nos. 32230006, 32200198, 32201881, and 31621001), the Southern University of Science and Technology (to X.W.D), and the Key Laboratory of Molecular Design for Plant Cell Factory of Guangdong Higher Education Institute (2019KSYS006).

Author contributions

Y.C., X.W.D., and J.L. designed the research and wrote the paper; Y.C., Y.L., X.L., M.Y., D.X., and J.L. performed experiments; Y.F. performed bioinformatic analysis; Y.C., Y.L., D.X., H.W., X.W.D., and J.L. analyzed data.

Supplemental data

The following materials are available in the online version of this article.

Supplemental Figure S1. The *myb112* mutants generated by CRISPR/Cas9.

Supplemental Figure S2. Hypocotyl phenotypes of Col-0, *myb112* mutants, and *MYB112* overexpression lines in darkness.

Supplemental Figure S3. Identification of transgenic plants overexpressing *MYB112*.

Supplemental Figure S4. Transcriptome analysis of *PIF1*, *PIF3*, *PIF5*, and *PIF7* expression in *myb112-4* and Col-0.

Supplemental Figure S5. MYB112 enhances the ability of PIF4 to activate the expression of *IAA19* and *IAA29*.

Supplemental Figure S6. MYB112 cannot directly bind to the promoter of *PIF4* or *YUCCA8* in Y1H assay.

Supplemental Figure S7. The *lux* mutant generated by CRISPR/Cas9.

Supplemental Figure S8. MYB112 transcript and protein levels during light-to-dark transition.

Supplemental Figure S9. *MYB112* is not a clock-regulated gene.

Supplemental Figure S10. Identification of *MYB112*$_{pro}$:*MYB112-GFP*/*myb112* transgenic lines.

Supplemental Data Set 1. Lists of genes whose expression is altered in the *myb112-4* mutant.

Supplemental Data Set 2. Primer sequences used in the study.

Supplemental Data Set 3. Summary of statistical analyses.

Conflict of interest statement. The authors declare no conflict of interest.

References

Al-Sady B, Ni W, Kircher S, Schäfer E, Quail PH. Photoactivated phytochrome induces rapid PIF3 phosphorylation prior to

proteasome-mediated degradation. Mol Cell. 2006:**23**(3):439–446. https://doi.org/10.1016/j.molcel.2006.06.011

Ballesteros ML, Bolle C, Lois LM, Moore JM, Vielle-Calzada J-P, Grossniklaus U, Chua N-H. LAF1, A MYB transcription activator for phytochrome A signaling. Gene Dev. 2001:**15**(19):2613–2625. https://doi.org/10.1101/gad.915001

Bauer D, Viczian A, Kircher S, Nobis T, Nitschke R, Kunkel T, Panigrahi KC, Adam E, Fejes E, Schafer E, et al. Constitutive photomorphogenesis 1 and multiple photoreceptors control degradation of phytochrome interacting factor 3, a transcription factor required for light signaling in *Arabidopsis*. Plant Cell. 2004:**16**(6):1433–1445. https://doi.org/10.1105/tpc.021568

Bernardo-García S, de Lucas M, Martínez C, Espinosa-Ruiz A, Davière J-M, Prat S. BR-dependent phosphorylation modulates PIF4 transcriptional activity and shapes diurnal hypocotyl growth. Gene Dev. 2014:**28**(15):1681–1694. https://doi.org/10.1101/gad.243675.114

Chen HM, Zou Y, Shang YL, Lin HQ, Wang YJ, Cai R, Tang XY, Zhou JM. Firefly luciferase complementation imaging assay for protein-protein interactions in plants. Plant Physiol. 2008:**146**(2):368–376. https://doi.org/10.1104/pp.107.111740

Chory J, Peto C, Feinbaum R, Pratt L, Ausubel F. *Arabidopsis thaliana* mutant that develops as a light-grown plant in the absence of light. Cell. 1989:**58**(5):991–999. https://doi.org/10.1016/0092-8674(89)90950-1

Christians MJ, Gingerich DJ, Hua Z, Lauer TD, Vierstra RD. The light-response BTB1 and BTB2 proteins assemble nuclear ubiquitin ligases that modify phytochrome B and D signaling in Arabidopsis. Plant Physiol. 2012:**160**(1):118–134. https://doi.org/10.1104/pp.112.199109

Christie JM, Arvai AS, Baxter KJ, Heilmann M, Pratt AJ, O'Hara A, Kelly SM, Hothorn M, Smith BO, Hitomi K, et al. Plant UVR8 photoreceptor senses UV-B by tryptophan-mediated disruption of cross-dimer salt bridges. Science. 2012:**335**(6075):1492–1496. https://doi.org/10.1126/science.1218091

Clough SJ, Bent AF. Floral dip: a simplified method for Agrobacterium -mediated transformation of *Arabidopsis thaliana*. Plant J. 1998:**16**(6):735–743. https://doi.org/10.1046/j.1365-313x.1998.00343.x

Deng XW, Caspar T, Quail PH. *Cop1*: a regulatory locus involved in light-controlled development and gene expression in *Arabidopsis*. Gene Dev. 1991:**5**(7):1172–1182. https://doi.org/10.1101/gad.5.7.1172

Dong J, Ni W, Yu R, Deng XW, Chen H, Wei N. Light-dependent degradation of PIF3 by SCF(EBF1/2) promotes a photomorphogenic response in *Arabidopsis*. Curr Biol. 2017:**27**(16):2420–2430. e2426. https://doi.org/10.1016/j.cub.2017.06.062

Dong J, Tang D, Gao Z, Yu R, Li K, He H, Terzaghi W, Deng XW, Chen H. Arabidopsis DE-ETIOLATED1 represses photomorphogenesis by positively regulating phytochrome-interacting factors in the dark. Plant Cell. 2014:**26**(9):3630–3645. https://doi.org/10.1105/tpc.114.130666

Dubos C, Stracke R, Grotewold E, Weisshaar B, Martin C, Lepiniec L. MYB transcription factors in *Arabidopsis*. Trends Plant Sci. 2010:**15**(10):573–581. https://doi.org/10.1016/j.tplants.2010.06.005

Earley KW, Haag JR, Pontes O, Opper K, Juehne T, Song K, Pikaard CS. Gateway-compatible vectors for plant functional genomics and proteomics. Plant J. 2006:**45**(4):616–629. https://doi.org/10.1111/j.1365-313X.2005.02617.x

Ezer D, Jung JH, Lan H, Biswas S, Gregoire L, Box MS, Charoensawan V, Cortijo S, Lai X, Stockle D, et al. The evening complex coordinates environmental and endogenous signals in *Arabidopsis*. Nat Plants. 2017:**3**(7):17087. https://doi.org/10.1038/nplants.2017.87

Ferrero V, Viola IL, Ariel FD, Gonzalez DH. Class I TCP transcription factors target the gibberellin biosynthesis gene GA20ox1 and the growth-promoting genes HBI1 and PRE6 during thermomorphogenic growth in *Arabidopsis*. Plant Cell Physiol. 2019:**60**(8):1633–1645. https://doi.org/10.1093/pcp/pcz137

Franklin KA, Lee SH, Patel D, Kumar SV, Spartz AK, Gu C, Ye S, Yu P, Breen G, Cohen JD, et al. Phytochrome-interacting factor 4 (PIF4) regulates auxin biosynthesis at high temperature. Proc Natl Acad Sci U S A. 2011:**108**(50):20231–20235. https://doi.org/10.1073/pnas.1110682108

Gao H, Song W, Severing E, Vayssières A, Huettel B, Franzen R, Richter R, Chai J, Coupland G. PIF4 enhances DNA binding of CDF2 to co-regulate target gene expression and promote Arabidopsis hypocotyl cell elongation. Nat Plants. 2022:**8**(9):1082–1093. https://doi.org/10.1038/s41477-022-01213-y

Hajdu A, Dobos O, Domijan M, Bálint B, Nagy I, Nagy F, Kozma-Bognár L. ELONGATED HYPOCOTYL 5 mediates blue light signalling to the Arabidopsis circadian clock. Plant J. 2018:**96**(6):1242–1254. https://doi.org/10.1111/tpj.14106

Han X, Yu H, Yuan R, Yang Y, An F, Qin G. Arabidopsis transcription factor TCP5 controls plant thermomorphogenesis by positively regulating PIF4 activity. iScience. 2019:**15**:611–622. https://doi.org/10.1016/j.isci.2019.04.005

Hazen SP, Schultz TF, Pruneda-Paz JL, Borevitz JO, Ecker JR, Kay SA. *LUX ARRHYTHMO* encodes a Myb domain protein essential for circadian rhythms. Proc Natl Acad Sci U S A. 2005:**102**(29):10387–10392. https://doi.org/10.1073/pnas.0503029102

Helfer A, Nusinow DA, Chow BY, Gehrke AR, Bulyk ML, Kay SA. *LUX ARRHYTHMO* encodes a nighttime repressor of circadian gene expression in the *Arabidopsis* core clock. Curr Biol. 2011:**21**(2):126–133. https://doi.org/10.1016/j.cub.2010.12.021

Hellens RP, Allan AC, Friel EN, Bolitho K, Grafton K, Templeton MD, Karunairetnam S, Gleave AP, Laing WA. Transient expression vectors for functional genomics, quantification of promoter activity and RNA silencing in plants. Plant Methods. 2005:**1**(1):13. https://doi.org/10.1186/1746-4811-1-13

Hellman LM, Fried MG. Electrophoretic mobility shift assay (EMSA) for detecting protein-nucleic acid interactions. Nat Protoc. 2007:**2**(8):1849–1861. https://doi.org/10.1038/nprot.2007.249

Herrero E, Kolmos E, Bujdoso N, Yuan Y, Wang M, Berns MC, Uhlworm H, Coupland G, Saini R, Jaskolski M, et al. EARLY FLOWERING4 recruitment of EARLY FLOWERING3 in the nucleus sustains the *Arabidopsis* circadian clock. Plant Cell. 2012:**24**(2):428–443. https://doi.org/10.1105/tpc.111.093807

Hong SH, Kim HJ, Ryu JS, Choi H, Jeong S, Shin J, Choi G, Nam HG. CRY1 inhibits COP1-mediated degradation of BIT1, a MYB transcription factor, to activate blue light-dependent gene expression in *Arabidopsis*. Plant J. 2008:**55**(3):361–371. https://doi.org/10.1111/j.1365-313X.2008.03508.x

Hornitschek P, Kohnen MV, Lorrain S, Rougemont J, Ljung K, Lopez-Vidriero I, Franco-Zorrilla JM, Solano R, Trevisan M, Pradervand S, et al. Phytochrome interacting factors 4 and 5 control seedling growth in changing light conditions by directly controlling auxin signaling. Plant J. 2012:**71**(5):699–711. https://doi.org/10.1111/j.1365-313X.2012.05033.x

Huai J, Zhang X, Li J, Ma T, Zha P, Jing Y, Lin R. SEUSS and PIF4 coordinately regulate light and temperature signaling pathways to control plant growth. Mol Plant. 2018:**11**(7):928–942. https://doi.org/10.1016/j.molp.2018.04.005

Huang W, Pérez-García P, Pokhilko A, Millar AJ, Antoshechkin I, Riechmann JL, Mas P. Mapping the core of the *Arabidopsis* circadian clock defines the network structure of the oscillator. Science. 2012:**336**(6077):75–79. https://doi.org/10.1126/science.1219075

Huq E, Quail PH. PIF4, a phytochrome-interacting bHLH factor, functions as a negative regulator of phytochrome B signaling in *Arabidopsis*. EMBO J. 2002:**21**(10):2441–2450. https://doi.org/10.1093/emboj/21.10.2441

Jiao Y, Lau OS, Deng XW. Light-regulated transcriptional networks in higher plants. Nat Rev Genet. 2007:**8**(3):217–230. https://doi.org/10.1038/nrg2049

Kamioka M, Takao S, Suzuki T, Taki K, Higashiyama T, Kinoshita T, Nakamichi N. Direct repression of evening genes by CIRCADIAN

CLOCK-ASSOCIATED1 in the *Arabidopsis* circadian clock. Plant Cell. 2016:**28**(3):696–711. https://doi.org/10.1105/tpc.15.00737

Lee SB, Kim HU, Suh MC. MYB94 and MYB96 additively activate cuticular wax biosynthesis in *Arabidopsis*. Plant Cell Physiol. 2016:**57**(11):2300–2311. https://doi.org/10.1093/pcp/pcw147

Lei Y, Lu L, Liu H-Y, Li S, Xing F, Chen L-L. CRISPR-P: a web tool for synthetic single-guide RNA design of CRISPR-system in plants. Mol Plant. 2014:**7**(9):1494–1496. https://doi.org/10.1093/mp/ssu044

Leivar P, Monte E, Al-Sady B, Carle C, Storer A, Alonso JM, Ecker JR, Quail PH. The *Arabidopsis* phytochrome-interacting factor PIF7, together with PIF3 and PIF4, regulates responses to prolonged red light by modulating phyB levels. Plant Cell. 2008a:**20**(2):337–352. https://doi.org/10.1105/tpc.107.052142

Leivar P, Monte E, Oka Y, Liu T, Carle C, Castillon A, Huq E, Quail PH. Multiple phytochrome-interacting bHLH transcription factors repress premature seedling photomorphogenesis in darkness. Curr Biol. 2008b:**18**(23):1815–1823. https://doi.org/10.1016/j.cub.2008.10.058

Leivar P, Quail PH. PIFs: pivotal components in a cellular signaling hub. Trends Plant Sci. 2011:**16**(1):19–28. https://doi.org/10.1016/j.tplants.2010.08.003

Li J, Terzaghi W, Gong YY, Li CR, Ling JJ, Fan YY, Qin NX, Gong XQ, Zhu DM, Deng XW. Modulation of BIN2 kinase activity by HY5 controls hypocotyl elongation in the light. Nat Commun. 2020:**11**(1):1592. https://doi.org/10.1038/s41467-020-15394-7

Lin C, Robertson DE, Ahmad M, Raibekas AA, Jorns MS, Dutton PL, Cashmore AR. Association of flavin adenine dinucleotide with the *Arabidopsis* blue light receptor CRY1. Science. 1995:**269**(5226):968–970. https://doi.org/10.1126/science.7638620

Liu H, Lin R, Deng XW. Photobiology: light signal transduction and photomorphogenesis. J Integr Plant Biol. 2020:**62**(9):1267–1269. https://doi.org/10.1111/jipb.13004

Lotkowska ME, Tohge T, Fernie AR, Xue GP, Balazadeh S, Mueller-Roeber B. The Arabidopsis transcription factor MYB112 promotes anthocyanin formation during salinity and under high light stress. Plant Physiol. 2015:**169**(3):1862–1880. https://doi.org/10.1104/pp.15.00605

Luo H, Laluk K, Lai Z, Veronese P, Song F, Mengiste T. The Arabidopsis Botrytis Susceptible1 Interactor defines a subclass of RING E3 ligases that regulate pathogen and stress responses. Plant Physiol. 2010:**154**(4):1766–1782. https://doi.org/10.1104/pp.110.163915

Ma D, Constabel CP. MYB repressors as regulators of phenylpropanoid metabolism in plants. Trends Plant Sci. 2019:**24**(3):275–289. https://doi.org/10.1016/j.tplants.2018.12.003

Makino S, Matsushika A, Kojima M, Oda Y, Mizuno T. Light response of the circadian waves of the APRR1/TOC1 quintet: when does the quintet start singing rhythmically in *Arabidopsis*? Plant Cell Physiol. 2001:**42**(3):334–339. https://doi.org/10.1093/pcp/pce036

Martinez-Garcia JF, Huq E, Quail PH. Direct targeting of light signals to a promoter element-bound transcription factor. Science. 2000:**288**(5467):859–863. https://doi.org/10.1126/science.288.5467.859

McNellis TW, Deng X-W. Light control of seedling morphogenetic pattern. Plant Cell. 1995:**7**(11):1749–1761. https://doi.org/10.1105/tpc.7.11.1749

Mengiste T, Chen X, Salmeron J, Dietrich R. The BOTRYTIS SUSCEPTIBLE1 gene encodes an R2R3MYB transcription factor protein that is required for biotic and abiotic stress responses in Arabidopsis. Plant Cell. 2003:**15**(11):2551–2565. https://doi.org/10.1105/tpc.014167

Millard PS, Kragelund BB, Burow M. R2r3 MYB transcription factors—functions outside the DNA-binding domain. Trends Plant Sci. 2019:**24**(10):934–946. https://doi.org/10.1016/j.tplants.2019.07.003

Mizuno T, Nakamichi N. *Pseudo*-response regulators (PRRs) or *true* oscillator components (TOCs). Plant Cell Physiol. 2005:**46**(5):677–685. https://doi.org/10.1093/pcp/pci087

Newman LJ, Perazza DE, Juda L, Campbell MM. Involvement of the R2R3-MYB, AtMYB61, in the ectopic lignification and dark-photomorphogenic components of the *det3* mutant phenotype. Plant J. 2004:**37**(2):239–250. https://doi.org/10.1046/j.1365-313X.2003.01953.x

Ni W, Xu SL, González-Grandío E, Chalkley RJ, Huhmer AFR, Burlingame AL, Wang ZY, Quail PH. PPKs mediate direct signal transfer from phytochrome photoreceptors to transcription factor PIF3. Nat Commun. 2017:**8**(1):15236. https://doi.org/10.1038/ncomms15236

Ni W, Xu SL, Tepperman JM, Stanley DJ, Maltby DA, Gross JD, Burlingame AL, Wang ZY, Quail PH. A mutually assured destruction mechanism attenuates light signaling in *Arabidopsis*. Science. 2014:**344**(6188):1160–1164. https://doi.org/10.1126/science.1250778

Nozue K, Covington MF, Duek PD, Lorrain S, Fankhauser C, Harmer SL, Maloof JN. Rhythmic growth explained by coincidence between internal and external cues. Nature. 2007:**448**(7151):358–361. https://doi.org/10.1038/nature05946

Nusinow DA, Helfer A, Hamilton EE, King JJ, Imaizumi T, Schultz TF, Farré EM, Kay SA. The ELF4-ELF3-LUX complex links the circadian clock to diurnal control of hypocotyl growth. Nature. 2011:**475**(7356):398–402. https://doi.org/10.1038/nature10182

Oh E, Zhu J-Y, Wang Z-Y. Interaction between BZR1 and PIF4 integrates brassinosteroid and environmental responses. Nat Cell Biol. 2012:**14**(8):802–809. https://doi.org/10.1038/ncb2545

Osterlund MT, Hardtke CS, Wei N, Deng XW. Targeted destabilization of HY5 during light-regulated development of *Arabidopsis*. Nature. 2000:**405**(6785):462–466. https://doi.org/10.1038/35013076

Park E, Kim Y, Choi G. Phytochrome B requires PIF degradation and sequestration to induce light responses across a wide range of light conditions. Plant Cell. 2018:**30**(6):1277–1292. https://doi.org/10.1105/tpc.17.00913

Park J, Nguyen KT, Park E, Jeon JS, Choi G. DELLA proteins and their interacting RING finger proteins repress gibberellin responses by binding to the promoters of a subset of gibberellin-responsive genes in Arabidopsis. Plant Cell. 2013:**25**(3):927–943. https://doi.org/10.1105/tpc.112.108951

Pham VN, Kathare PK, Huq E. Phytochromes and phytochrome interacting factors. Plant Physiol. 2018a:**176**(2):1025–1038. https://doi.org/10.1104/pp.17.01384

Pham VN, Xu XS, Huq E. Molecular bases for the constitutive photomorphogenic phenotypes in *Arabidopsis*. Development. 2018b:**145**(23):dev169870. https://doi.org/10.1242/dev.169870

Pucciariello O, Legris M, Costigliolo Rojas C, Iglesias MJ, Hernando CE, Dezar C, Vazquez M, Yanovsky MJ, Finlayson SA, Prat S, et al. Rewiring of auxin signaling under persistent shade. Proc Natl Acad Sci U. S. A. 2018:**115**(21):5612–5617. https://doi.org/10.1073/pnas.1721110115

Rizzini L, Favory JJ, Cloix C, Faggionato D, O'Hara A, Kaiserli E, Baumeister R, Schafer E, Nagy F, Jenkins GI, et al. Perception of UV-B by the *Arabidopsis* UVR8 protein. Science. 2011:**332**(6025):103–106. https://doi.org/10.1126/science.1200660

Robinson MD, McCarthy DJ, Smyth GK. Edger: a bioconductor package for differential expression analysis of digital gene expression data. Bioinformatics. 2009:**26**(1):139–140. https://doi.org/10.1093/bioinformatics/btp616

Schaffer R, Ramsay N, Samach A, Corden S, Putterill J, Carré IA, Coupland G. The *late elongated hypocotyl* mutation of Arabidopsis disrupts circadian rhythms and the photoperiodic control of flowering. Cell. 1998:**93**(7):1219–1229. https://doi.org/10.1016/S0092-8674(00)81465-8

Sharrock RA, Quail PH. Novel phytochrome sequences in *Arabidopsis thaliana*: structure, evolution, and differential expression of a plant regulatory photoreceptor family. Gene Dev. 1989:**3**(11):1745–1757. https://doi.org/10.1101/gad.3.11.1745

Shen Y, Khanna R, Carle CM, Quail PH. Phytochrome induces rapid PIF5 phosphorylation and degradation in response to red-light activation. Plant Physiol. 2007:**145**(3):1043–1051. https://doi.org/10.1104/pp.107.105601

Shi H, Lyu M, Luo Y, Liu S, Li Y, He H, Wei N, Deng XW, Zhong S. Genome-wide regulation of light-controlled seedling morphogenesis by three families of transcription factors. Proc Natl Acad Sci U S A. 2018:**115**(25):6482–6487. https://doi.org/10.1073/pnas.1803861115

Shin J, Kim K, Kang H, Zulfugarov IS, Bae G, Lee CH, Lee D, Choi G. Phytochromes promote seedling light responses by inhibiting four negatively-acting phytochrome-interacting factors. Proc Natl Acad Sci U S A. 2009:**106**(18):7660–7665. https://doi.org/10.1073/pnas.0812219106

Shin J, Park E, Choi G. PIF3 regulates anthocyanin biosynthesis in an HY5-dependent manner with both factors directly binding anthocyanin biosynthetic gene promoters in *Arabidopsis*. Plant J. 2007:**49**(6):981–994. https://doi.org/10.1111/j.1365-313X.2006.03021.x

Silva CS, Nayak A, Lai X, Hutin S, Hugouvieux V, Jung JH, Lopez-Vidriero I, Franco-Zorrilla JM, Panigrahi KCS, Nanao MH, et al. Molecular mechanisms of evening complex activity in *Arabidopsis*. Proc Natl Acad Sci U S A. 2020:**117**(12):6901–6909. https://doi.org/10.1073/pnas.1920972117

Stracke R, Ishihara H, Huep G, Barsch A, Mehrtens F, Niehaus K, Weisshaar B. Differential regulation of closely related R2R3-MYB transcription factors controls flavonol accumulation in different parts of the *Arabidopsis thaliana* seedling. Plant J. 2007:**50**(4):660–677. https://doi.org/10.1111/j.1365-313X.2007.03078.x

Stracke R, Turgut-Kara N, Weisshaar B. The AtMYB12 activation domain maps to a short C-terminal region of the transcription factor. Z Naturforsch C. 2017:**72**(7–8):251–257. https://doi.org/10.1515/znc-2016-0221

Su C, Wang Y, Yu Y, He Y, Wang L. Coordinative regulation of plants growth and development by light and circadian clock. aBIOTECH. 2021:**2**(2):176–189. https://doi.org/10.1007/s42994-021-00041-6

Sun J, Qi L, Li Y, Chu J, Li C. PIF4–mediated Activation of *YUCCA8* expression integrates temperature into the auxin pathway in regulating *Arabidopsis* hypocotyl growth. PLoS Genet. 2012:**8**(3):e1002594. https://doi.org/10.1371/journal.pgen.1002594

Sun J, Qi L, Li Y, Zhai Q, Li C. PIF4 And PIF5 transcription factors link blue light and auxin to regulate the phototropic response in *Arabidopsis*. Plant Cell. 2013:**25**(6):2102–2114. https://doi.org/10.1105/tpc.113.112417

Sun Q, Wang S, Xu G, Kang X, Zhang M, Ni M. SHB1 And CCA1 interaction desensitizes light responses and enhances thermomorphogenesis. Nat Commun. 2019:**10**(1):3110. https://doi.org/10.1038/s41467-019-11071-6

Vierstra RD, Quail PH. Purification and initial characterization of 124-kilodalton phytochrome from *Avena*. Biochemistry. 1983:**22**(10):2498–2505. https://doi.org/10.1021/bi00279a029

Wang Z-P, Xing H-L, Dong L, Zhang H-Y, Han C-Y, Wang X-C, Chen Q-J. Egg cell-specific promoter-controlled CRISPR/Cas9 efficiently generates homozygous mutants for multiple target genes in *Arabidopsis* in a single generation. Genome Biol. 2015:**16**(1):144. https://doi.org/10.1186/s13059-015-0715-0

Wang Z-Y, Tobin EM. Constitutive expression of the *CIRCADIAN CLOCK ASSOCIATED 1 (CCA1)* gene disrupts circadian rhythms and suppresses its own expression. Cell. 1998:**93**(7):1207–1217. https://doi.org/10.1016/S0092-8674(00)81464-6

Xu X, Yuan L, Yang X, Zhang X, Wang L, Xie Q. Circadian clock in plants: linking timing to fitness. J Integr Plant Biol. 2022:**64**(4):792–811. https://doi.org/10.1111/jipb.13230

Yan Y, Li C, Dong X, Li H, Zhang D, Zhou Y, Jiang B, Peng J, Qin X, Cheng J, et al. MYB30 is a key negative regulator of Arabidopsis photomorphogenic development that promotes PIF4 and PIF5 protein accumulation in the light. Plant Cell. 2020:**32**(7):2196–2215. https://doi.org/10.1105/tpc.19.00645

Zhang B, Holmlund M, Lorrain S, Norberg M, Bakó L, Fankhauser C, Nilsson O. BLADE-ON-PETIOLE proteins act in an E3 ubiquitin ligase complex to regulate PHYTOCHROME INTERACTING FACTOR 4 abundance. eLife. 2017:**6**:e26759. https://doi.org/10.7554/eLife.26759

Zhang Y, Cao G, Qu L-J, Gu H. Characterization of *Arabidopsis* MYB transcription factor gene *AtMYB17* and its possible regulation by LEAFY and AGL15. J Genet Genomics. 2009:**36**(2):99–107. https://doi.org/10.1016/S1673-8527(08)60096-X

Zhou Y, Xun Q, Zhang D, Lv M, Ou Y, Li J. TCP transcription factors associate with PHYTOCHROME INTERACTING FACTOR 4 and CRYPTOCHROME 1 to regulate thermomorphogenesis in *Arabidopsis thaliana*. iScience. 2019:**15**:600–610. https://doi.org/10.1016/j.isci.2019.04.002